An empirical ship domain based on evasive maneuver and perceived collision risk

Lei Du[1], Osiris A. Valdez Banda[1], Yamin Huang[2,3], Floris Goerlandt[4], Pentti Kujala[1], Weibin Zhang[5,*]

[1] Aalto University, School of Engineering, Department of Mechanical Engineering, Espoo, Finland
[2] National Engineering Research Center for Water Transport Safety (WTS), Wuhan, China
[3] Wuhan University of Technology, Intelligent Transportation System Research Center, Wuhan, China
[4] Dalhousie University, Department of Industrial Engineering, Halifax, Nova Scotia, B3H 4R2, Canada
[5] School of Electronic and Optical Engineering, Nanjing University of Science and Technology, Nanjing, 210094, China

Abstract

This paper introduced a new ship domain concept and an analytical framework. The ship domain takes the point of the ship's first evasive maneuver as a basis and correlates it with the navigator-perceived collision risk level. The first evasive maneuver of a ship is detected based on the ship turning point identification and ship intention estimation. The available maneuvering margin (AMM) is utilized as a proxy to measure the perceived collision risk by the navigator. Interpreting the first evasive maneuver in terms of this AMM over a large sample of vessel encounters taken from automatic identification system (AIS) data finally enables an empirical estimation of the size of this ship domain. The method is applied to AIS data in the Northern Baltic Sea, and separate ship domains are constructed for the give-way and stand-on vessels with different maneuverability characteristics. Compared to the existing proximity-based ship domain, this ship domain explicitly incorporates the dynamic nature of the encounter process and the navigator's evasive maneuvers. Several advantages of this proposed ship domain concept and limitations of the presented modeling approach are discussed. Finally, possible future applications are explained, including waterway safety assessment and navigational decision support systems to reduce ship-ship collision risk.

Keywords: Maritime safety; Ship maneuverability; Ship domain; AIS data; Velocity obstacle; Ship-ship collision

1. Introduction

Ship collision, as one of the most frequently occurring accidents at sea (Kujala et al., 2009; Du et al., 2020b and 2021; Zhang et al., 2020), has attracted significant attention in academic research. In the past decades, various concepts and techniques have been proposed for preventing ship collision accidents or analyzing their spatio-temporal occurrence patterns and risks in waterways (Valdez Banda et al., 2015, 2019; Szlapczynski and Szlapczynska, 2016; Zhang et al., 2016; Fan et al., 2020; Kulkarni et al., 2020; Gil et al., 2019 and 2020; Zhu et al., 2020; Rong et al., 2021). However, the occurrence of marine casualties and incidents remains stable at a high level (EMSA, 2020).

The timing when a ship takes evasive maneuvers is critical for the success of collision avoidance. Many methods have been proposed to help navigators find the proper timing for collision avoidance actions. For instance, the last time to take action (LTTA) (Zhuo and Tang, 2008), the minimum distance to collision (MDTC) (Montewka et al., 2010, 2014), the last line of defense (LLoD) (Baldauf et al., 2017) have been adopted to inform the navigator of imminent danger. Szlapczynski et al. (2018) combine ship maneuverability and ship domain (SD) to determine the last moment when a particular collision avoidance maneuver can still be successfully performed. By using this approach, the critical condition for a ship to take evasive action is quantified, beyond which a collision cannot be avoided. There are many studies on the construction of a collision alert system (CAS) to alert the ship to act properly (Baldauf et al., 2011; Simsir et al., 2014; Goerlandt et al., 2015). However, their applicability is limited by certain assumptions made to simplify the encounter process, such as the ship sailing in a straight line with constant speed. Other work has focused on the concept of the SD as an area which the navigator would like to keep clear from other ships, for navigational safety reasons, see Szlapczynski and Szlapczynska (2017) for a recent review. Such domains are typically defined based on proximity information, i.e., on the distance between the vessels in the encounter, see e.g., Hansen et al. (2013) and Zhang and Meng (2019) for empirically estimated domains based on AIS data. While many SD formulations have been proposed, these originate from the idea that a certain area around a vessel needs to be clear from other vessels, based on ideas originally presented by Goodwin (1975). However, these existing SDs cannot be utilized as a critical criterion with direct application in collision avoidance (Montewka et al., 2020). Therefore, efforts are still required on how to assist navigators to perform maneuvers for collision avoidance based on these existing SDs.

Existing research attests that the timing of ship taking evasive maneuvers is primarily affected by the risk perceived by the navigator (Chauvin and Lardjane 2008; Kim 2020). In this work, the navigator-perceived risk refers to their understanding and tolerance of a collision, which depends on their experience, their understanding of the regulations, and the difficulty in performing evasive maneuvers for collision avoidance. Hence, in this article, a new concept of a ship domain is proposed, based on the timing of evasive maneuvering to avoid a ship-ship collision, which is associated with the perceived risk level at the time of taking such an evasive maneuver.

The risks intuitively perceived by the navigator are normally interpreted from Automated Radar Plotting Aid (ARPA) information (Statheros et al., 2008) by setting some critical values based on the navigators' understanding of ship maneuverability or even company rules, etc. Information, such as the Distance at Closest Point of Approach (DCPA) and Time to Closest Point of Approach (TCPA) plays a key role in this assessment. The perceptions of risk may vary for different navigators (Nicholas, 2006) and many methods have been proposed to analyze factors affecting the perceived risk of collision (Aydogdu et al., 2010; Zhang et al., 2019; Kim, 2020). The pilot-perceived collision risk has been used by Chin and Debnath (2009) as a basis for developing a collision alert system. The stakeholders' perception of risk has been measured by a generic fuzzy analytical hierarchy process method (Aydogdu, 2014). Nonetheless, there is currently no SD concept which is defined based on the relationship between the collision risk perceived by the navigator and the timing of taking action for collision avoidance.

Inspired by the techniques for constructing an empirical SD, such as those used by Pedersen et al. (2013) and Zhang and Meng (2019), statistical features of the collision risk level as perceived by the navigator at the time when the evasive maneuver is initiated can be obtained from AIS data. The concept of available maneuvering margins (AMM) developed in (Du et al., 2020c; Huang and van Gelder, 2020) is adopted as a proxy for the navigator-perceived risk when the ship starts to take evasive maneuvers, for two reasons. First, the perceived risk of a conflict relates strongly to the level of handling difficulty forced on the mariner (Inoue, 2000). When navigators manipulate a ship, its responsiveness is restricted by its maneuverability (Hong and Yang, 2012). Second, risk measures independent of conflict resolution may lead to inaccurate detection of actual danger (Chen et al., 2018). Under the same circumstances, ships with a higher AMM have a greater possibility of eliminating risks, so the risks are relatively lower. However, this is not often taken into consideration (Du et al., 2020c).

Therefore, the aims of this article are two-fold. First, to measure the risk perceived by the navigator, a risk perception-based SD is proposed based on the concept of AMM. Second, the boundary of this SD concept is empirically determined based on historical AIS data, utilizing various models to interpret vessel encounters in terms of the timing of evasive maneuvers and the navigator-perceived collision risk. This proposed SD is a practical SD that reveals under what conditions the navigator will start to maneuver for collision avoidance. The conception and construction of this novel SD provides new insights into the behavior of navigators in collision avoidance contexts. The utilization of this risk perception-based SD can support collision detection and conflict resolution. Specifically, this risk perception-based SD can help navigators to understand the collision risk and prompts them to prepare evasive maneuvers for collision avoidance. This also can help the traffic management authorities understand the traffic risks and then some instructions can be made to guide the ship maneuver. Therefore, this contribute to a reduction in ship collisions and the improvement of water traffic management through various possible applications of this domain concept.

The remainder of this work is arranged as follows. Section 2 consists of a literature review on the existing research about the SD. Section 3 explains the methodology of building this SD. Case studies are introduced in Section 4 to demonstrate the proposed methodology using AIS data from the Northern Baltic Sea. Discussion and conclusions are addressed in Section 5 and Section 6, respectively.

2. Literature review on ship domain

The SD, which has a profound impact on modern navigation technology, was proposed in the 1970s for estimating waterway capacity. Fujii and Tanaka (1971) observed from radar data that most navigators would avoid entering a certain region around a vessel, and this region was defined as the SD. Based on their work, various types of SD have been developed, and some major changes are briefly highlighted below (Figure 1). A comprehensive review of SD and its applications can be found in Szlapczynski and Szlapczynska, 2017.

First, the probabilistic boundary of the domain was developed. In the early stage, the boundary of the domain was deterministic, e.g., in (Goodwin, 1975). Thus, when we apply the domain in collision alarms, the collision risk only has two values, 1 or 0 (i.e., violation or not), which differs from the interpretation of navigators. Zhao et al. (1993) then explained the SD by analogy with the personal space from physiology and introduced a fuzzy SD with a probabilistic boundary. This idea was widely accepted, and many researchers developed probabilistic domains, see for example papers by (Gucma and Marcjan, 2012, Zhang and Meng, 2019), etc.

Second, the data-based SD has been intensively studied in recent years. The original SD was based on offshore radar, e.g. papers by (Coldwell, 1983, Fujii and Tanaka, 1971). Later on, many researchers modified the original SD by incorporating experts' knowledge (Zhu et al., 2001). For instance, Goodwin (1975) suggested three-section domains, incorporating the responsibilities of the ship addressed in International Regulations for Preventing Collisions at Sea (COLREGs, 1972). Kijima and Furukawa (2003) adopted a two semi-ellipse domain concerning ship maneuverability, where the two semi-ellipses share the same short axis. Wang (2010) formulated a quaternion SD that consists of four quarter-ellipses (or triangles). In brief, over a period of time, modifications based on the original SD that incorporated experts' knowledge were popular. However, in recent years, due to the spreading of AIS (Mou et al., 2010), researchers have gained a powerful tool to investigate the SD from the perspective of the ship. Since then, many researchers have proposed a new form of the SD, e.g. (Hansen et al., 2013, Zhang and Meng, 2019).

Third, the dynamic SD was developed for collision prevention. The static SD is helpful for capacity estimation, but not for dynamic collision prevention since working conditions are time-varying. To fill the gap, one group of researchers developed a series of static SDs and chose the most appropriate one in for corresponding working conditions (Pietrzykowski, 2008), e.g., open sea or restricted area (Wielgosz, 2017), different courses (Pietrzykowski and Uriasz, 2008), different encounter types (Coldwell, 1983, Fiskin et al., 2020), etc. Another group of researchers employed motion simulations in the construction of the domain (or distance), e.g., MDTC (Montewka et al., 2012), action lines (Szlapczynski et al., 2018), etc. For instance, Gil et al. (2020) simulated two-ship encounters and identified the region surrounding one ship that the other ship needs to take action before violating and this region is also called the "critical area".

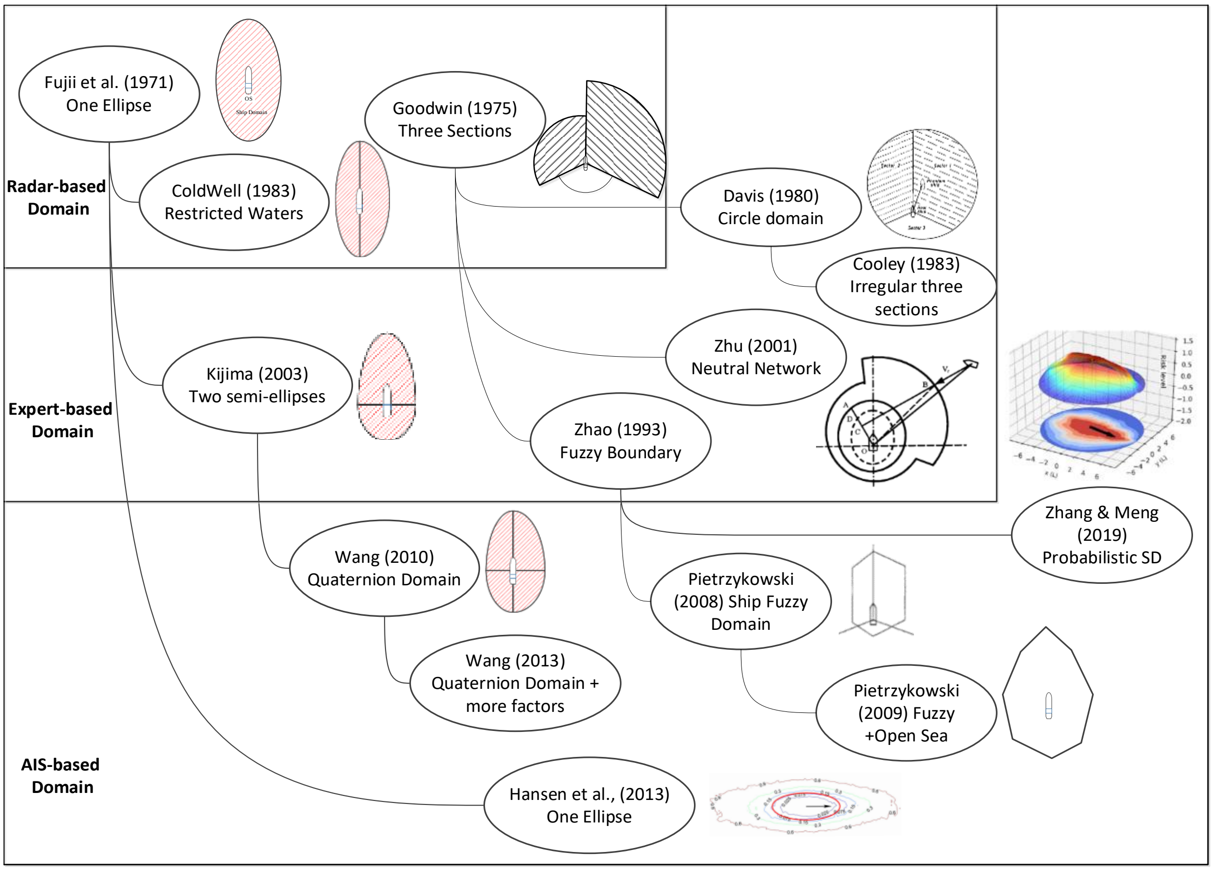

Figure. 1 Typical ship domains to illustrate the development of its application in collision prevention

From the development of the SD, we can clearly see that the purpose of the SD switches from capacity estimation (or waterway safety assessment) to collision avoidance, specifically, e.g., conflict precaution (finding the moment in time to pay attention to approaching dangers), and collision avoidance alarm (finding the moment in time to take evasive actions), etc. To determine the time for taking evasive actions, the performance of the ship avoiding collision should be evaluated, otherwise, the alarm might result in the under-estimation of risk (Huang and Gelder, 2020). However, most SDs neglect this aspect. Thus, the AMM is introduced to evaluate the performance of the ship avoiding collision in each encounter, with the aim of offering a new tool for the construction of the SD.

3. Methodology

The key to the construction of this risk perception-based SD is to link the timing of the ship taking evasive maneuvers with the corresponding perceived risk by the navigator. This involves three aspects. First, ship conflict needs to be detected. Second, it needs to be determined at what point a ship takes evasive maneuvers to avoid a ship-ship collision. Third, the navigator's perceived risk level at that point in time when evasive action is undertaken needs to be estimated. In this context, the COLREGs need to be considered, as these are the background for navigators' interpretation of ship encounter situations. Combining the three above steps using a set of data mining and analysis algorithms will enable the empirical estimation of this SD.

The detection of ship conflict can be easily obtained as various methods have been proposed (Gil et al., 2020; Du et al., 2019). However, it is difficult to determine when a ship takes evasive maneuvers for conflict elimination. The link of the actions and the ship intention is a challenge. During the process of conflict elimination, the ship can take many actions for multiple purposes. The method of ship intention estimation proposed in Du et al., (2020a) helps find a ship's evasive maneuvers. The second challenge is the extraction of an indicator that can reflect characteristics of the navigator's perceived risk when the ship responds to the conflict. The concept of AMM reflects the capacity of resolving a conflict in terms of how many maneuvering options leads to a successful conflict elimination compared to how many options there are available, as developed in (Du et al., 2020c; Huang and van Gelder, 2020). Therefore, the concept of AMM is adopted here.

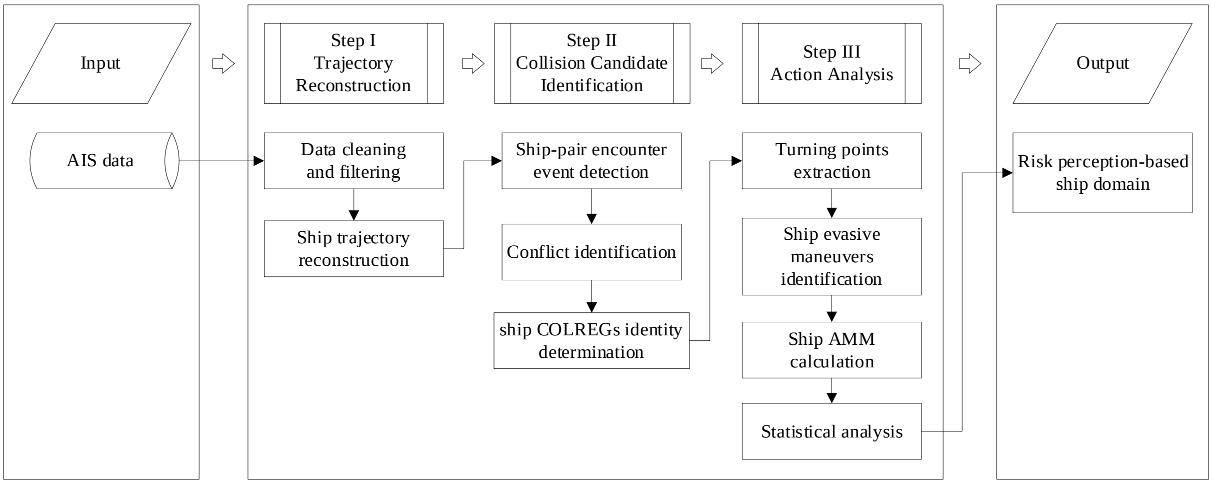

Figure 2 The method proposed for constructing risk perception-based ship domain

The entire process of constructing a risk perception-based SD is presented in Figure 2.

Step I: Reconstructing ship trajectories from AIS data. This step extracts the sailing information of each ship from the raw AIS data. After data cleaning and filtering, some errors are deleted. Then, the trajectory of the ship is reconstructed based on a linear interpolation so that it is updated at each same time step.

Step II: Identifying collision candidates, i.e., pairs of ships in conflict. This step identifies all the ships that have a conflict with each other from historical AIS data, which contains (1) the ship-pair encounter event detection, (2) conflict identification, and (3) ship COLREGs identity determination.

Step III: Ship action analysis is employed to find the moment when the ship takes evasive maneuvers for conflict elimination. This process includes extraction of turning points by the Douglas–Peucker (DP) algorithm, identification of ship evasive maneuvers by ship intention estimation based on non-linear velocity obstacles (NLVO) algorithm, and the calculation of AMM. For each pair of collision candidates, the AMM value when the ship starts to take evasive maneuvers is recorded and statistically analyzed for the construction of a collision risk perception-based SD.

3.1 Step I: Trajectory reconstruction

AIS data consists of static and dynamic messages from each ship and the database stores the messages in chronological order of receipt. To obtain the trajectory of each ship, the database needs to be re-sorted by MMSI number and then the messages belonging to the same ship are updated by the time series. Hence, the trajectory of the ship is obtained.

Many factors can affect AIS data quality. The raw AIS data contains noise and error information, including ship position errors and abnormal speeds (Zhang et al., 2018). Therefore, these incorrect ship trajectories are deleted after data cleaning and filtering (Zhang et al., 2015).

The time interval of AIS broadcasts varies, so the AIS data could be interpolated with a predefined time interval. In that case, a linear interpolation method is employed, and the predefined time interval is set to one minute.

3.2 Step II: Collision candidate identification

3.2.1 Ship-pair encounter event detection

It is beneficial to analyze a conflict from the perspective of regarding a ship-pair encounter as a process (Chen et al., 2018). Hence, the concept of ship-pair encounter event (SPEE) is employed. An SPEE signifies the process of an encounter between a ship pair within a specified time period. Each SPEE is given a number of attributes, relevant for conflict assessment.

The SPEE can be detected by the following two steps. The first is the determination of a ship pair encountering each other. The targeted ship pair refers to a ship pair whose minimum relative distance between them is less than the distance limit Dis_{Limit}. The second step is the determination of the time period t_{SPEE}. This work focuses on the ship's first evasive maneuver. Many ships may maneuver for collision avoidance quite early to control the situation (Robert et al., 2003; Chauvin and Lardjane, 2008). To avoid missing the real first evasive maneuver, t_{SPEE} is preliminarily determined as a consecutive one-hour period, which is half an hour before and after the moment of closest point of approach (CPA). Then, the distance limit is employed to shorten this time period to limit the computation time.

$$t_{\min Dis} - 30 \le t_{SPEE} \le t_{\min Dis} + 30 \,\&\, Dis(t_{SPEE}) \le Dis_{Limit}, \tag{1}$$

where $t_{\min Dis}$ is the moment of CPA. Dis_{Limit} is set as 12 nm as it is the normal radar range setting (Juszkiewicz, 2016). The sailing information of one ship in one SPEE is $data(t_{SPEE}) = \{Lon(t_{SPEE}), Lat(t_{SPEE}), v(t_{SPEE}), c(t_{SPEE}), h(t_{SPEE})\}$. Lon (°) and Lat (°) are the longitude and latitude, respectively. v (kn) is the ship speed, c (°) is the ship course, and h (°) is the ship heading.

3.2.2 Conflict identification

The NLVO algorithm considers the dynamic nature of ship action throughout the encounter process (Huang et al., 2017), and therefore it is employed to improve the accuracy of conflict identification.

$$IC(t_r) = \begin{cases} 1, \ if \ \ V_{TS}(t_r) \cap S_{NL\_VO}(t_r) \ne \varnothing, t_r \in t_{SPEE} \\ 0, \ \text{else} \end{cases}, \tag{2}$$

where IC represents the conflict index, S_{NL_VO} is the velocity obstacle (VO) zone in the velocity space of the target ship, see the red marked area in Figure 3. The formula derivation process of S_{NL_VO} is elaborated in Huang et al., 2017. $\varnothing$ is the empty set. If the TS's velocity V_{TS} falls in the VO zone S_{NL_VO}, $IC = 1$ and a conflict exists, see V_1 in Figure 3. Otherwise, there is no conflict, see V_2 in Figure 3. t_r is the time when the conflict exists. The simulation time for conflict detection is limited by t_{SPEE}. More details are provided in Du et al., 2020c. Through this formula, the conflict between each SPEE is identified.

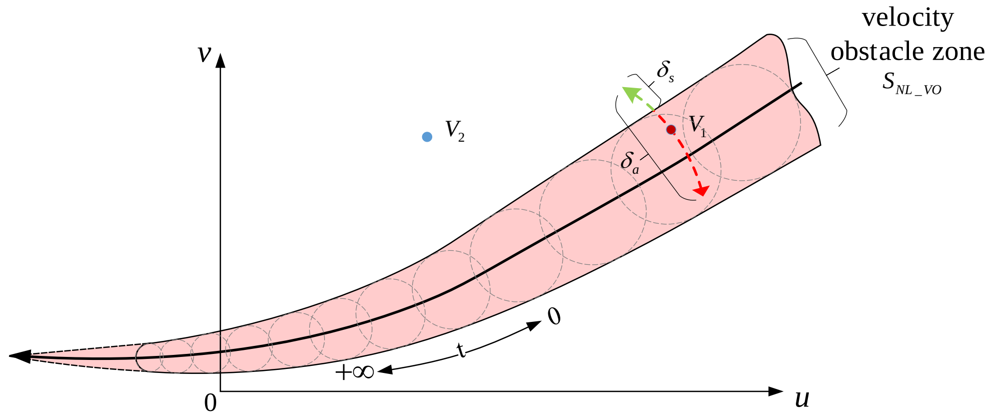

Figure 3 Collision risk detection based on NL-VO algorithm

3.2.3 Ship COLREGs identity determination

The ship COLREGs identity is classified in terms of its action obligation for conflict elimination, which includes the give-way ship (GW) and the stand-on ship (SO). The ship COLREGs identity is determined according to their relative bearing (RB) and relative heading (RH) (COLREGs, 1972). In Figure 4, the RB and RH of the target ship (TS) seen from the own ship (OS) are divided into eight sectors, adopted from Tam and Bucknall, 2010 and Goerlandt et al., 2015. The OS is located in the center of Figure 4.

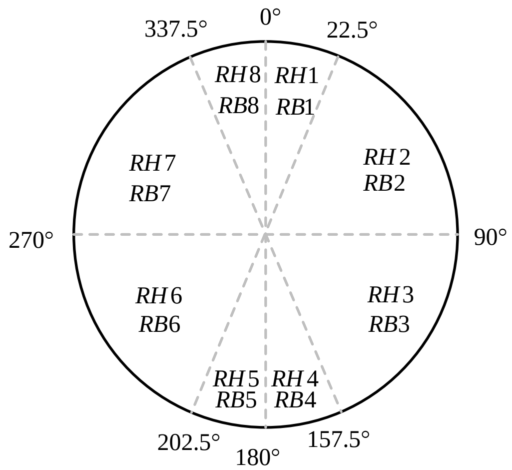

Figure 4 Regions used for the encounter type categorization and ship COLREGs identity determination, adapted from Tam and Bucknall, 2010 and Goerlandt et al., 2015

Table1. Ship COLREGs identity of OS in different encounter types, adapted from Tam and Bucknall, 2010 and Goerlandt et al., 2015

Ship COLREGs identity	RH1	RH2	RH3	RH4	RH5	RH6	RH7	RH8
RB1	OT	SF	CR/SO	CR/SO	HO/GW	CR/GW	CR/GW	OT
RB2	OT	SF	SF	SF	CR/GW	CR/GW	CR/GW	OT
RB3	OT	SF	SF	SF	SF	CR/GW	CR/GW	OT
RB4	OT	SF	SF	SF	SF	SF	CR/GW	OT
RB5	OT	CR/SO	SF	SF	SF	SF	SF	OT
RB6	OT	CR/SO	CR/SO	SF	SF	SF	SF	OT
RB7	OT	CR/SO	CR/SO	CR/SO	CR/GW	SF	SF	OT
RB8	OT	CR/SO	CR/SO	HO/GW	CR/GW	CR/GW	SF	OT

In Table 1, the combinations of these sectors determine the ship COLREGs identity of OS in different types of encounter. Overtaking (OT), Head-On (HO), and Crossing (CR) refer to different encounter types. SF means safe passing. For the OT, ship COLREGs identity is determined by her speed. The OS is SO if the speed of the OS is lower than that of the TS, otherwise, the OS is the GW. For instance, in Table 1, if a TS is located in RB2 with a relative heading of RH6, then the OS is the GW in a crossing encounter scenario.

3.3 Step III: Ship action analysis

3.3.1 Ship turning points extraction

We assume that a ship only alters her course for conflict elimination with the ship speed unchanged, based on statistical analysis (Baldauf et al., 2017). The turning points are where the ship alters her course.

The DP algorithm (Douglas and Peucker, 1973) has been widely adopted in the compression of ship trajectory data (Zhao and Shi, 2018), due to its accuracy and efficiency in simplifying the trajectory. Therefore, the DP algorithm with a reasonable compression threshold can be utilized as a simplification method for ship trajectories to identify the ship turning points (Du et al., 2020a). The sailing information of one ship of each SPEE can be simplified as $data(t_{tp}) = \left\{Lon(t_{tp}), Lat(t_{tp}), v(t_{tp}), c(t_{tp}), h(t_{tp})\right\}, t_{tp} \subseteq t_{SPEE}$. t_{tp} is the turning time identified by the DP algorithm. The compression threshold is set as 15 m based on the sensitivity analysis, as described in Du et al., 2020a.

3.3.2 First evasive maneuver identification

The ship may adopt evasive maneuvers several times for conflict elimination. This work aims to explore the feature of perceived risk that triggers navigators to take evasive maneuvers. Therefore, the focus of this work is the first evasive maneuver.

In Du et al., 2020a, the evasive maneuver is that the ship changes her course or/and speed to eliminate a conflict. By utilizing the NLVO algorithm, the evasive maneuver can be identified by checking whether there is a conflict when the ship is at a turning point.

$$\begin{cases} V_{TS}(t_{ea}) \cap S_{NL\text{-VO}}(t_{ea}) \neq \varnothing, t_{ea} \in t_{tp} \\ t_1 = \min(t_{ea}) \end{cases}, \tag{3}$$

where t_{ea} indicates the time that the ship takes an evasive maneuver. At t_{ea}, the ship makes a turn and the conflict exists. t_1 is the first time that the ship takes an evasive maneuver.

3.3.3 Ship AMM calculation

To present the risk perceived by the navigator, the concept of AMM has been adopted as an indicator. The AMM is measured based on the proportion of maneuvers by which the OS can eliminate conflicts, to all its available maneuvers (Du et al., 2020c):

$$\begin{cases} AMM(t_1) = \dfrac{\sum \delta_s(t_1)}{\delta_a(t_1)}, \ if \ \exists V_{OS}(t_1) \in RV_{OS}(\delta_s(t_1), t_{ob}): V_{OS}(t_1) \cap S_{NL\_VO}(t_1) = \varnothing \\ t_{ob} = \max(TCPA, 5) \end{cases}, \tag{4}$$

where $AMM(t_1)$ is the value of AMM when the ship starts to act to eliminate the conflict at t_1. $AMM(t_1)$ ranges from 0 to 1. A higher $AMM(t_1)$ means that the ship has more space and time to execute a maneuver, and hence a higher chance of avoiding a dangerous encounter. δ_s is the value of the adopted rudder angle that can eliminate the existing conflict, see the dotted arc in green color in Figure 3. δ_a is all the rudder angles available to the OS and $-35° \leq \delta_a \leq 35°$, see the dotted arc in Figure 3. $RV_{OS}(\delta_s(t_1), t_{ob})$ is the OS's reachable velocity after steering with a demanded rudder angle δ_s within the observation time t_{ob}, which is determined by her current velocity $V_{TS}(t_r)$ and her turning ability, see Du et al., 2020a. The turning ability of a ship is modeled based on the Nomoto model (Nomoto et al., 1956). Two key parameters (i.e., K and T) are determined as $\mathrm{K} = 2K_0 \cdot V_{OS} / L_{OS}$ and $\mathrm{T} = 2K_0 \cdot L_{OS} / V_{OS}$ (Hong & Yu, 2000). Here, we have $K_0 = 1.5$ and $T_0 = 2.5$ for the passenger and cargo ship, and $K_0 = 1.5$ and $T_0 = 6$ for the tanker (Hong & Yu, 2000). The Time to Closest Point of Approach (TCPA) is adopted to determine the observation time t_{ob}. The minimum value of t_{ob} is set as five minutes in order to have sufficient observation time.

3.3.4 Statistical analysis

For each SPEE at risk of conflict, the calculated AMM value when the ship starts to take an evasive maneuver is recorded. Afterwards, the statistical analysis of AMM is performed for the construction of the risk perception-based SD.

Regarding the shape of this SD, it should be analyzed by visualizing the value of AMM in intensity plots. The AMM intensity plots are generated based on the value of AMM and the relative bearing between this ship pair in polar coordinates.

For the size of this SD, the curve of its boundary should be interpreted in such a way that the entire area outside this curve has an intensity greater than the value indicated on the level curve. In this work, the value of the boundary of this SD is determined by the analysis of ship behavior characteristics.

4. Case study

A profile of marine traffic from AIS data is illustrated in Section 4.1, followed by the detection of ship encounters from AIS data in Section 4.2. The analysis of each SPEE is explained in detail by introducing two typical scenarios in Section 4.3, and the risk perception-based SD from the SO and the GW perspectives are presented in Section 4.4. Lastly, the comparison of risk perception-based SD from the GW and the SO perspectives is addressed in Section 4.5.

4.1 Ship profiles in AIS database

In this section, the proposed method for determining the risk perception-based SD is applied to the Northern Baltic Sea area, which is defined as the Baltic Sea with a latitude exceeding 59°N. In our work, we did not start from raw AIS data. The AIS data adopted in this work had already been processed by Zhang et al. (2015 and 2016). The raw AIS data of these studies originally came from HELCOM (2012). After data processing, including cleaning, filtering and interpolation, this AIS data was applied to detect any possible near misses in the Northern Baltic Sea, as discussed in Zhang et al., 2015 and 2016, and Du et al., 2021. The promising results attest that the quality of this AIS data is acceptable. AIS data from the Northern Baltic Sea in July 2011 was used (Figure 5).

One-month voyage data from AIS data consisted of 2757 ships, including specific purpose ships, such as tugs, pilot vessels, wing in ground, high-speed craft, and dredgers. These specific purpose ships, including tugs, pilot vessels, wing in ground, high-speed craft, and dredgers were excluded because their working states are not recorded in the AIS data. Their behaviors in working and non-working states are different (Zhou et al., 2019) due to their different responsibilities for taking evasive action, as specified in Rule 18 of COLREGs. Therefore, this work only investigates the following three types of ships: passenger ships, tankers, and cargo ships. As a result, there were 1638 ships in total, of which around 61.8% were cargo ships (1012), 16% passenger ships (262), and 22.2% tankers (364). The average length of the passenger ships, tankers, and cargo ships were 95.6 m, 153.2 m, and 123.9 m, respectively.

The navigator-perceived risk may vary with the size of the ship as maneuverability diminishes as the vessel size increases (Pérez and Clemente, 2007). Therefore, ships are further divided into three categories. The length of a small-size ship is less than 100 m and the length of a medium-size ship ranges from 100 m to 200 m. The rest are categorized as large-size ships (above 200 m).

Additionally, there are two assumptions in this work for the determination of a ship's COLREGs identity. The first is that all of the ships are considered to be power-driven ships. Therefore, the ship COLREGs identity of each ship can be determined based on their relative position and relative heading. The second assumption is that the visibility in the summertime (July 2011) in the Northern Baltic Sea is good, which is an assumption also made in Kujala et al. (2009) and Asmi et al. (2011). Hence, Rules 11 to 18 in COLREGs are applicable.

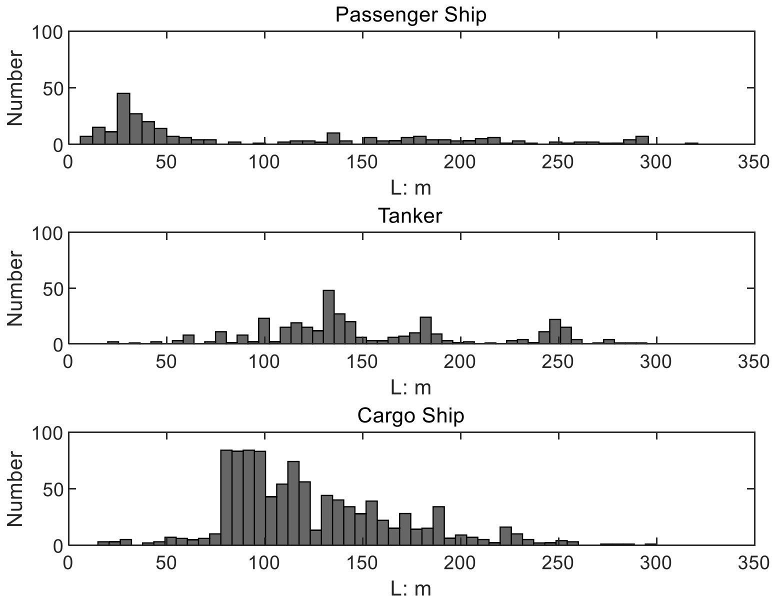

Figure 5 Size of ship in the Northern Baltic Sea from the AIS database

4.2 Detection of Ship-pair Encountering Events from AIS data

By adopting the methods described in Section 3.2.1, 30344 SPEEs were detected. More than 26% of these encounters (7969 encounters) presented a conflict through the method mentioned in Section 3.2.2. The ship COLREGs identity, i.e., either GW or SO, was also identified using the method in Section 3.2.3. For HO, both ships should turn to starboard for safe passing, according to COLREGs. Hence, both ships were regarded as GW.

Table 2 shows the number of GW and SO belonging to different ship types and ship lengths in all SPEEs with conflict. For passenger ships, most of the encountering ship lengths were small. Passenger ships were considered a GW and an SO 2474 times and 2227 times, respectively. For tankers, it was mostly medium size ships that appeared mostly in the studied region. 723 tankers were classified as GW, and 689 tankers as SO. For cargo ships, most of the ship's lengths were less than 200 m, i.e., small and medium size. The cargo ships were GW and SO 1761 times and 1686 times, respectively.

Table 2 The counts of GW and SO belonging to different ship types and ship length in all SPEEs with conflict, resulting from the method in Section 3.2.2 and Second 3.2.3

Ship Length	Passengers		Tankers		Cargo ships	
	GW	SO	GW	SO	GW	SO
Small	1201	1145	91	93	493	560
Medium	801	689	533	526	1168	1049
Large	472	396	99	70	100	77

4.3 Demonstration of analyzing SPEEs for the construction of risk perception-based SD

Two typical encounter scenarios were selected from the AIS data to demonstrate the process of analyzing SPEEs. The results of the encounter process analysis from the GW perspective are discussed in Section 4.3.1 and Section 4.3.2. The ship attributes are shown in Table 3. The encountering processes are illustrated in Figures 6 and 7, in which the line in black is the trajectory of the SO and that of the GW is colored. Four figures for each encounter scenario are introduced to demonstrate the process in Figures 6 and 7. Figure 6(a) and 7(a) show the layout of the whole encounter process, and some results of the analysis are highlighted. Specifically, the result of collision risk analysis, turning point identification, evasive action extraction, and the AMM value at the moment when the first evasive action is taken are presented. The blue circle on the GW's trajectory is the GW's position when the GW turns, and the black circle is the position of the SO when the GW takes action. The red solid dot shows the position of the two ships when the ships reach the Closest Point of Approach (CPA) (the position where the ship is identified as being in danger by traditional methods). The arrows at the ends indicate the ending points of the ship trajectory. Figures 6(b) and 7(b) focus on the conflict development process, where the ship heading and course are shown. Figures 6(c) and 7(c) present the ship course and course change, and the ship heading and heading change as the conflict develops. Figures 6(d) and 7(d) show the relative distance between the ship pair during the conflict development process. In this work, the relative distance between the ship pair is the Euclidean distance between the ship positions. The black line represents the relative distance between the ship pair and the blue circle on this black line indicates when the GW makes a turn.

Table 3. Ship attributes in three typical encounter scenarios

Ship attributes	COLREGs identity	MMSI	Type	Length (m)	Width m
Scenario 1	GW	27335xxxx	Tanker	81	14
	SO	27343xxxx	Tanker	125	16
Scenario 2	GW	31158xxxx	Passenger ship	290	30
	SO	26552xxxx	Passenger ship	38	8

The results of the encounter analysis are collected in Table 4. Table 4 shows the time when the conflict exists, when the ship makes a turn, when the ship pair reaches the CPA, and when the ship takes an evasive maneuver. The red marked area means the moment that the conflict exists, and the blue marked area means when the situation became safe. (t_{rs}, t_{re}) is the starting and ending moment of the conflict. $(t_{TP}, \Delta C)$ is the time the ship was turning and the amount of course change. $\Delta C > 0$ means the ship turns to starboard, and $\Delta C < 0$ refers to a portside turn. t_{CPA} is the time when this ship pair arrives at CPA. t_{ea} is the time when the ship takes an evasive maneuver. The unit of time is a minute, and the unit of course change is a degree.

Table 4. Result of the encounter process analysis of three encounter events

SPEEs	(t_{rs}, t_{re})	$(t_{TP}, \Delta C)$									t_{CPA}	t_{ea}
Scenario 1	(22, 30)	15, 25.6	21, -11.9	27, -15.1	41, -21.5						30	27
Scenario 2	(1, 21)	6, -14.9	8, -4.5	12, -13.8	14, -7.5	20, -3.1	25, 13.4	26, 1.8	34, 10.7	39, -2.7	18	6, 8, 12, 14, 20

Note: The red marked area means that a conflict exists, and the blue marked area means it is safe. A negative course change refers to a portside turn and a positive number refers to a starboard side turn. The unit of time is a minute and that of the course change is a degree.

4.3.1 Scenario 1

Figure 6 presents the result of Scenario 1 from a GW perspective. The encounter duration t_{SPEE} was 61 min. The conflict was detected from 22 min to 30 min.

The GW took actions four times during the whole encounter process (Figure 6(a)). First of all, the GW ship turned to starboard around 25.6° at 15 min (Figure 6(c), Table 4). This turn did not generate a conflict and the GW would safely pass the SO ship's stern if this sailing state remained. The second turn happened at 21 min, when the ship turned to port around 11.8° (Figure 6(c), Table 4). The second turn re-caused the conflict from 22 min. To eliminate the conflict, the GW turned 15.1° to port at 27 min. The ship pair continued to approach each other and the relative distance between them dropped to 0.315 nm at the CPA (Figure 6(d)). Afterwards, the ship pair gradually moved apart from each other and the conflict was over at 30 min. The fourth turn at 41 min was to further extend the relative distance between them for safety.

The third turn that occurred at 27 min was determined as an evasive maneuver (Figure 6(b)), when the AMM of GW was 88.6%. Thus, for this SPEE, we infer that the ship could bear the risk until the AMM fell to 88.6%. More details can be seen in Table 4.

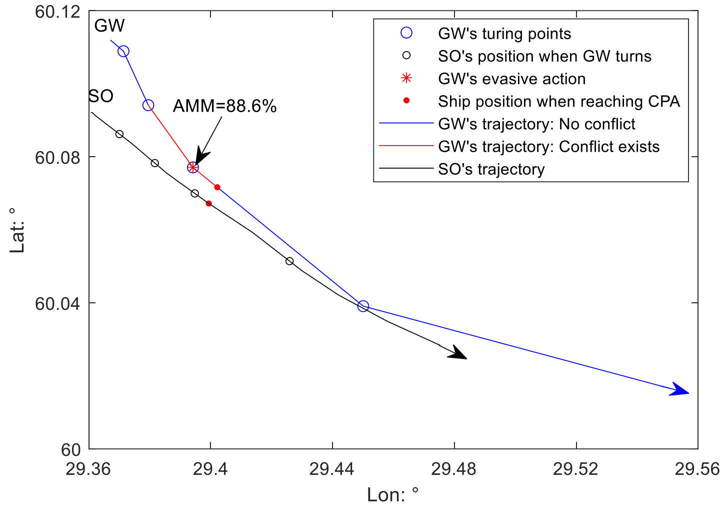

GW
SO
AMM=88.6%
GW's turing points
SO's position when GW turns
GW's evasive action
Ship position when reaching CPA
GW's trajectory: No conflict
GW's trajectory: Conflict exists
SO's trajectory
60.12
60.08
60.04
60
Lat: °
29.36
29.4
29.44
29.48
29.52
29.56
Lon: °

(a)

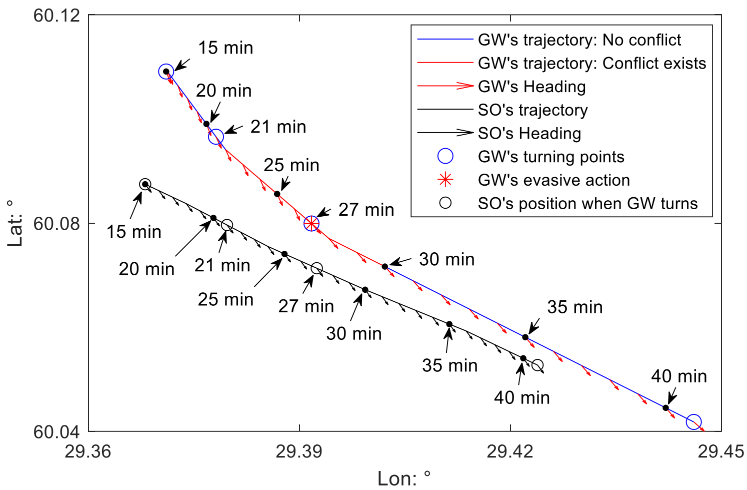

GW's trajectory: No conflict
GW's trajectory: Conflict exists
GW's Heading
SO's trajectory
SO's Heading
GW's turning points
GW's evasive action
SO's position when GW turns
15 min
20 min
21 min
25 min
27 min
30 min
35 min
40 min
15 min
20 min
21 min
25 min
27 min
30 min
35 min
40 min
60.12
60.08
60.04
Lat: °
29.36
29.39
29.42
29.45
Lon: °

(b)

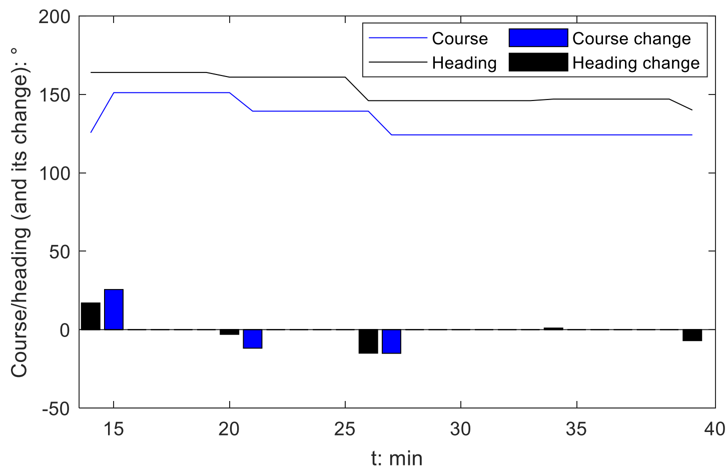

Course
Heading
Course change
Heading change
200
150
100
50
0
-50
Course/heading (and its change): °
15
20
25
30
35
40
t: min

(c)

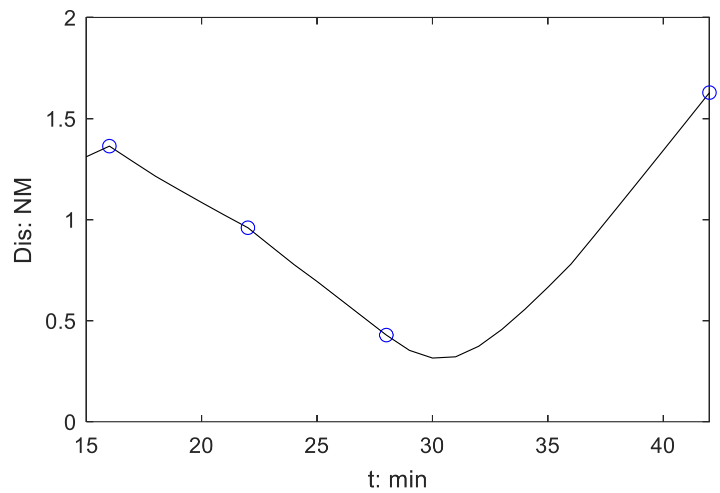

(d)

Figure 6 Illustration of the AMM calculation for the SPEE from the GW perspective in Scenario 1

4.3.2 Scenario 2

Figure 7 shows the results of Scenario 2. The duration of this crossing encounter was 45 min. From the GW perspective, this ship pair experienced a conflict before 21 min.

In this case, eight turns from the GW ship were detected (Figure 7(a)). The GW first turned around 14.9° to port at 6 min, with the aim of avoiding the conflict with the SO. This action was not sufficient, so the conflict still existed. To eliminate the conflict, the GW turned left several times (Figure 7(c), Table 4), such as the turn at 8 min (-4.5°), 12 min (-13.8°), 14 min (-7.5°) and 20 min (-3.1°). At 18 min, their relative distance fell to the lowest, around 0.11 nm (Figure 7(d)). After 18 min, their relative distance increased and there was no conflict after 21 min. The following turns of the GW at 25 min, 26 min, 34 min, and 39 min aimed to increase their relative distance and return to its original track.

The five actions of the GW at 6 min, 8 min, 12 min, 14 min, and 20 min were evasive maneuvers (Figure 7(b)). Since the first evasive maneuver was taken at 6 min when the AMM of the GW was 37.1% (Figure 7(a)), we infer that the ship could bear the risk until the AMM fell to 37.1%. More details can be seen in Table 4.

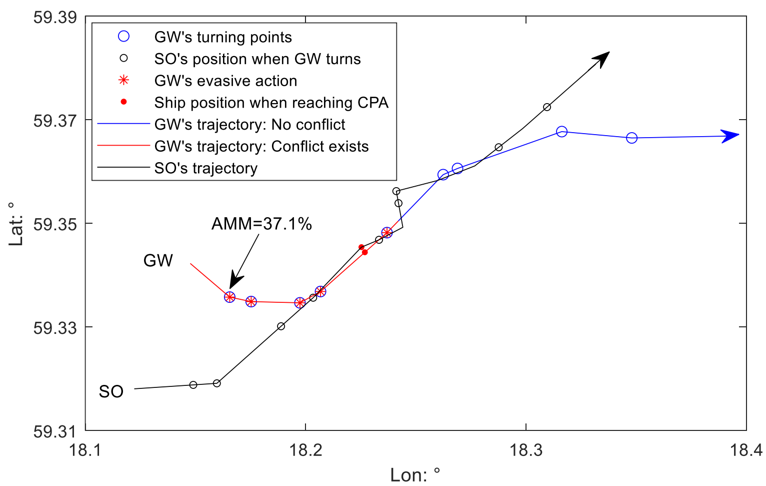

(a)

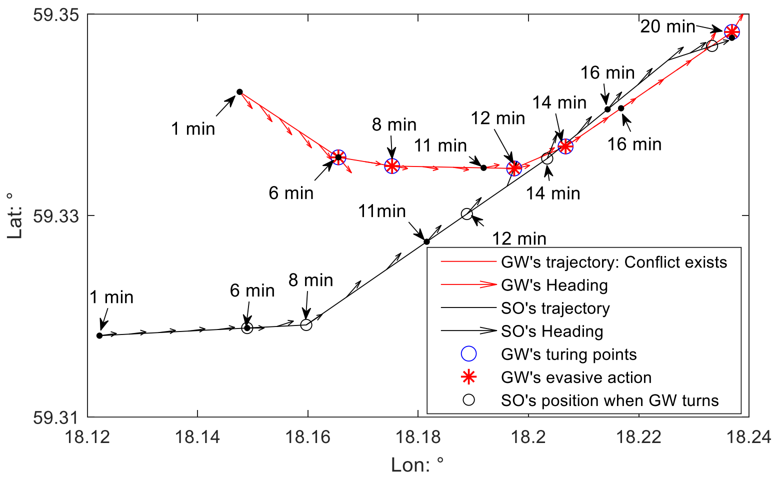

(b)

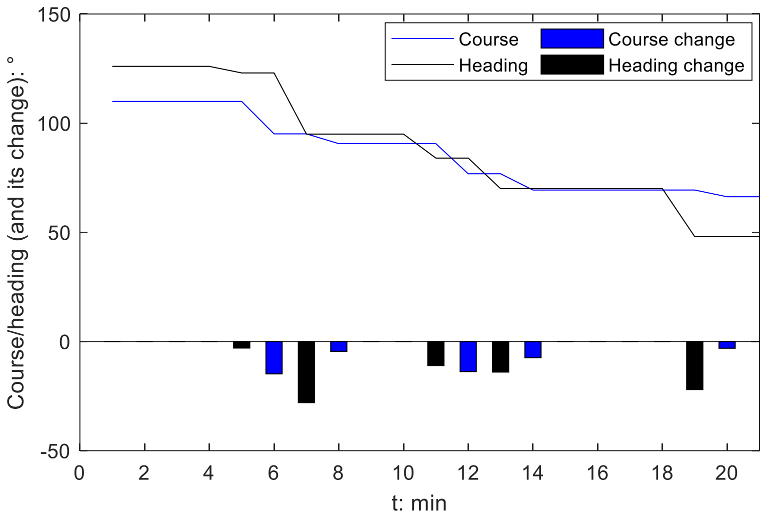

(c)

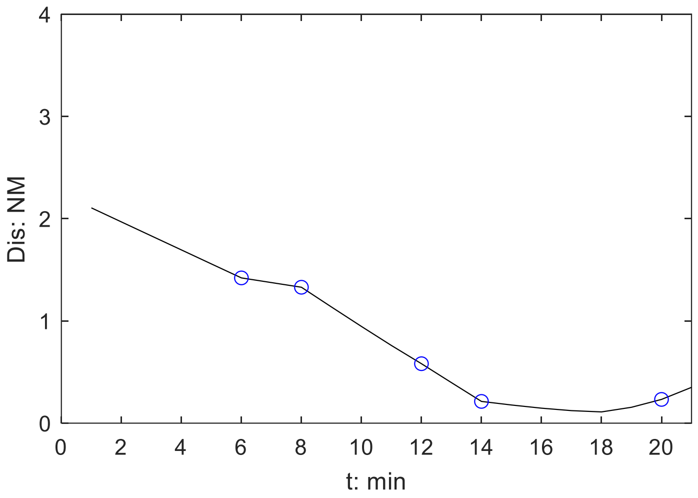

(d)

Figure 7 Illustration of the AMM calculation for the SPEE from the GW perspective in Scenario 3

4.4 Risk perception-based SD from different perspectives

The boundary of the risk perception-based SD is determined based on the statistical analysis of the AMM of each ship when a ship starts to take evasive maneuver. The impact of a ship COLREG identity on ship behavior is also considered in this work.

4.4.1 Give-way ship's risk perception-based SD

Figure 8 visualizes the AMM value of the GW the moment at which the GW starts to take an evasive maneuver, in two different modes. Figure 8(a) presents a histogram and Figure 8(b) shows a polar diagram.

Figure 8(a) presents the result in a histogram, where the x-axis shows the AMM value and the y-axis indicates the ratio of the GW taking actions at different AMM levels. From Figure 8(a), we can observe that most GWs take actions when the AMM is still at a high level, which implies that the GW would take actions early, once dangers were detected.

Furthermore, the timing for taking actions differs for ships of different lengths. Approximately 95% of GW passenger ships, which are small in size, start to take evasive maneuvers before the AMM drops to 0.92. If we set AMM = 0.95 as a threshold, 93.6% of small-size passenger ships will take action, while this rate drops to 87.1% and 77.3% for medium- and large-size passenger ships. Likewise, we can observe a similar pattern for the tankers and cargo ships. From the data, we can conclude that smaller size ships take actions earlier than larger size ships.

Figure 8(b) uses a polar diagram to explain the data. Each gray point represents one record. The length of the point indicates the AMM level when the GW starts to take evasive maneuvers, the angle of which indicates the RB of this ship pair at that moment from the OS perspective. The OS is located in the origin and points to the 0°. By analyzing each dangerous encounter, we constructed scatter plots.

Furthermore, we simplified the shape of the risk perception-based SD as a circular shape by visually analyzing the value of the GW's AMM in intensity plots in Figure 8(b). We added a circle at the origin in the diagram, which cuts the diagram into two parts and the radius of the circle is the AMM level. The points inside the circle mean the ships take actions after the AMM drops to the pre-set AMM level.

Let us set 90% as a threshold to determine the boundary of risk perception-based SD, inspired by the work done by Hörteborn et al., 2019. Then the circle that excludes 90% of the ships can be found, which is the circular risk perception-based SD**,** see the red ring in the figure. 90% of the points beyond the red ring and the point inside the ring imply some unusual cases where action was taken later than in the other 90% of the cases. The AMM values of the boundary of the risk perception-based SD for different ships are listed in Table 5.

- When a passenger ship is the GW and of small, medium, or large size, the boundary of the risk perception-based SD is AMM=0.986, 0.914, and 0.814, respectively.
- When a tanker is the GW and of small, medium, or large size, the boundary of the risk perception-based SD is AMM=0.843, 0.829, and 0.8, respectively.
- When a cargo ship is the GW and of small, medium, or large size, the boundary of risk perception-based SD is AMM=0.9, 0.886, and 0.871, respectively.

- These results demonstrate that not only the ship length but also the type of ship affects the navigator-perceived risk. The boundary of the risk perception-based SD of passenger ships is larger than that of the other two ship types. One possible cause is that passenger ships have stricter requirements for safe operations. Therefore, passenger ships usually take evasive maneuvers early to eliminate any potential risk. As a GW, the boundary of risk perception-based SD of a tanker is generally smaller than that of a cargo ship. We discuss possible causes of this phenomenon in Section 5.1.

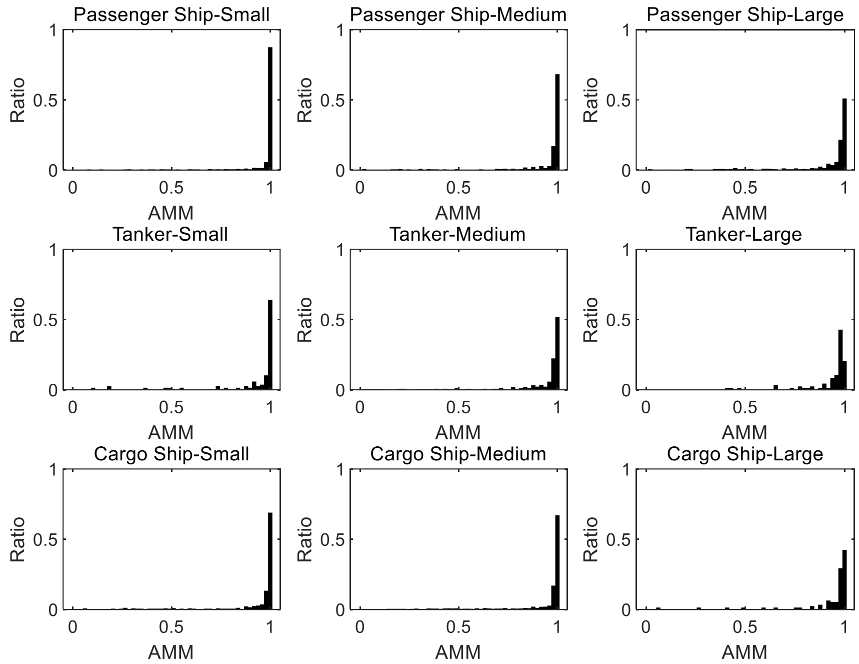

(a) Statistical histogram of AMM of GW

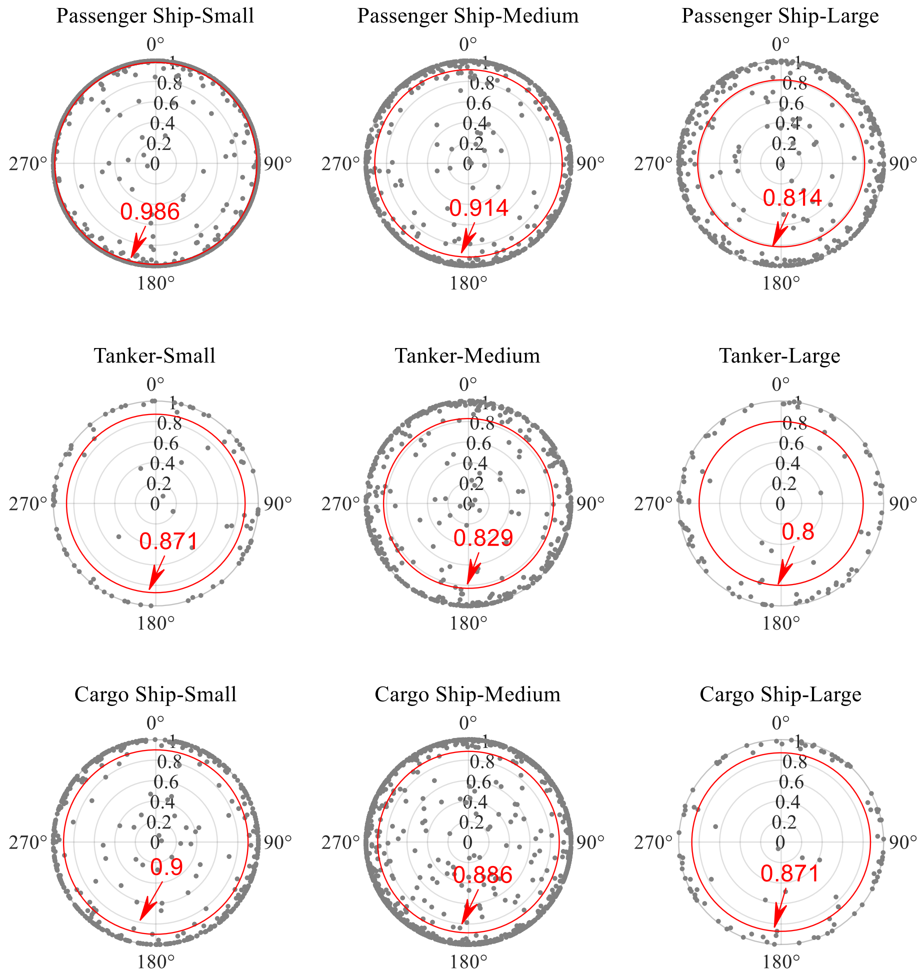

(b) The polar coordinate diagram of GW's AMM value and its risk perception-based SD

Figure 8 Visualization of the AMM value of GW when the GW starts to take evasive maneuver

4.4.2 Stand-on ship's risk perception-based SD

Figure 9 presents the result of the SO's AMM when the SO starts to act for conflict elimination. Figure 9(a) is a statistical histogram and Figure 9(b) is a polar coordinate diagram.

Similarly to Figure 8(a), the x-axis in Figure 9(a) is the AMM value when the SO starts to take evasive maneuvers and its y-axis indicates the ratio of the SOs that take actions at different AMM levels. In Figure 9(a), most of the SOs also prefer to take collision avoidance actions early, when their AMM is still at a high level, so as to master the situation, which is consistent with the findings in Chauvin and Lardjane, 2008. This can be supported by the fact that approximately 95.8% of the small-size passenger ships start to take evasive maneuvers before the AMM decreases to 0.8. Before the AMM drops to 0.8, almost 90% of the small-size tanker ships and 88% of the small-size cargo ships have started to take actions to avoid conflict.

Furthermore, the timing for ships of different lengths to take evasive maneuvers is also different. Specifically, the AMM when the SO starts to take evasive maneuvers decreases as the ship size increases. About 95% of SO passenger ships of small, medium, and large size begin to take evasive maneuvers before AMM drops to 0.829, 0.5 and 0.486 respectively.

AMM = 0.95 is set as the threshold, below which the rate of a small-size oil tanker that is the SO starts to take evasive maneuvers is 77.4%, while that decreases to 72.2% for medium size and 38.5% for large size. This similar trend holds true for cargo ships. For a cargo ship that is the SO, the percentage of ships starting to take evasive maneuver is 78.8% for small-size, 72.7% for medium-size, and 71.8% for the large-size group.

Figure 9(b) shows a polar coordinate diagram that presents the SO AMM value when the evasive maneuver starts. The angular coordinate and the radius of the polar coordinate diagram have the same meaning as in Figure 8(b). We also simplified the shape of the risk perception-based SD to make it circular. Its boundary is the critical AMM value before which 90% of the ships will act, which is indicated by the red circle in each polar coordinate diagram in Figure 9(b). The size of the risk perception-based SD is affected by the ship size. The AMM values of the boundary of the risk perception-based SD for different ships are listed in Table 5.

- When a passenger ship is the SO and of small, medium or large size, the boundary of risk perception-based SD is AMM=0.943, 0.786, and 0.729, respectively.
- When a tanker is the SO and of small, medium or large size, the boundary of risk perception-based SD is AMM=0.857, 0.629, and 0.486, respectively.
- When a cargo ship is the SO in small, medium or large size, the boundary of risk perception-based SD is AMM=0.729, 0.5, and 0.486, respectively.

Further, we observed that the size of the risk perception-based SD of the SO was different for different types of ship. Generally, when being as the SO, the size of the risk perception-based SD of a passenger ship is larger than that of a tanker, which is larger than that of a cargo ship. We discuss the possible causes in Section 5.1.

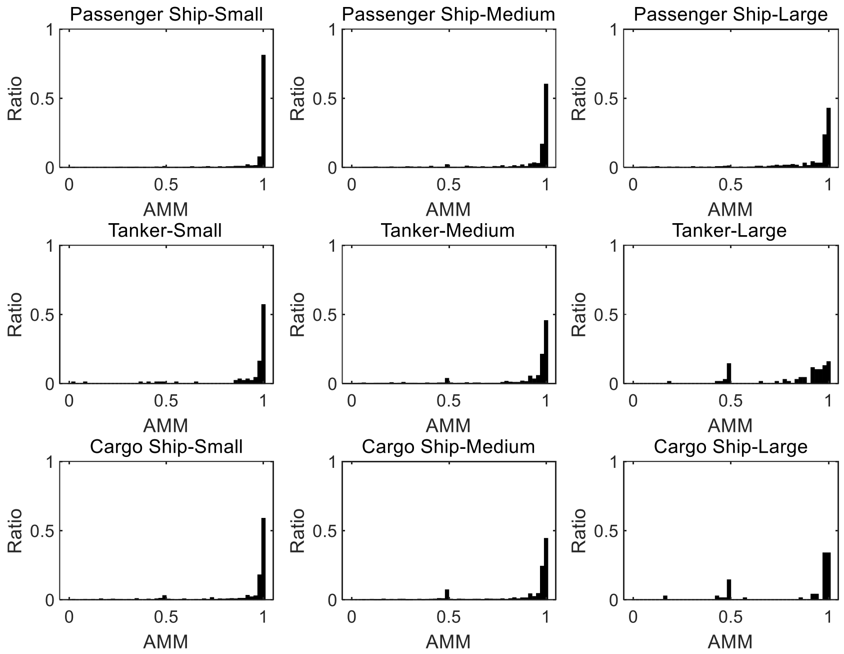

(a) Statistical histogram of AMM of SO

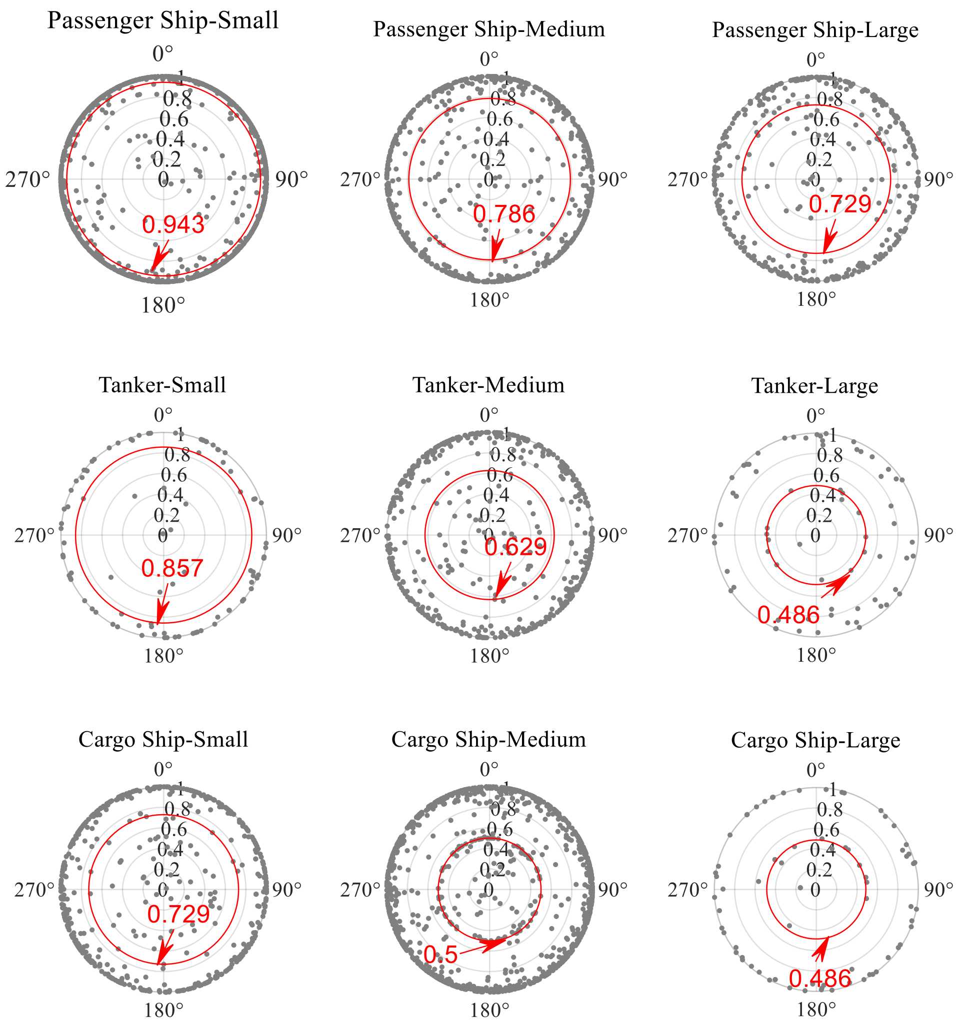

(b) The polar coordinate diagram of SO's AMM value and its risk perception-based SD

Figure 9 Visualization of the AMM value of SO when the SO starts to take evasive maneuver

4.5 Comparison between the risk perception-based SD of GW and OS

The size of risk perception-based SD of a ship whose identity is GW is generally larger than that of a ship whose identity is SO (see Table 5). When being as the SO, ships are more inclined to let the GW respond, and therefore their time to act is relatively late. For instance, for a large-size passenger ship, the AMM value at the boundary of risk perception-based SD is 0.814 for being as a GW and 0.729 for being as an SO. For a large-size tanker, whose identity is SO, the AMM value at the boundary of risk perception-based SD is 0.486, while the value is 0.8 for a tanker whose identity is GW. For a large-size cargo ship that is the SO, the AMM value at the boundary of the risk perception-based SD is 0.486, while the value is 0.871 when it is the GW. More details can be seen in Table 5.

Table 5. The AMM value at the boundary of risk perception-based SD for different ships

Ship type		Small	Medium	Large
Passenger Ship	GW	0.986	0.914	0.814
	SO	0.943	0.786	0.729
Tanker	GW	0.871	0.829	0.8
	SO	0.857	0.629	0.486
Cargo Ship	GW	0.9	0.886	0.871
	SO	0.729	0.5	0.486

5. Discussion

5.1 The feature of risk perception-based SD

Based on the present analysis, we found that the proposed risk perception-based SD has the following features:

First, the ship's COLREGs identity affects the size of the risk perception-based SD, see Figures 8 and 9. The size of the risk perception-based SD of a GW ship is larger than that of a SO ship (Table 5). The rules as specified in COLREGs provide a possible explanation. The GW and SO have different action responsibilities during different encounter stages, see Rules 16, 17, and 18 in COLREGs, 1972. When a conflict exists, the SO is not allowed to act to avoid conflict at the onset of the encounter. The SO can, however, take an evasive maneuver when the conflict becomes serious due to the GW's improper strategy of conflict elimination. Therefore, the SO seems to be more likely to let the GW respond first, waiting to initiate collision avoidance actions until the navigator of the SO vessel believes the risk levels become too high and action is required. Nevertheless, a common feature of the risk perception-based SD of both GW and SO vessels is that navigators prefer to act early. This is in accordance with the provisions of the COLREGs and earlier research findings (Robert et al., 2003; Chauvin and Lardjane, 2008). This widely adopted strategy of conflict elimination (Olsson and Jansson, 2006) aims at mastering the interaction situations, leading to fewer very close near misses (Belcher, 2003).

Second, the size of the risk perception-based SD decreases with increasing ship sizes, see Figures 8 and 9. In the present analysis, ships are divided into three groups based on their length. From the results shown in Section 4.4, smaller ships take actions earlier than larger ships. For instance, for a passenger ship being as an SO, the AMM at the boundary of its risk perception-based SD is 0.943 for small-size vessels, which drops to 0.786 for medium-size and 0.729 for large-size, see Table 5. This shows that navigators of larger ships prefer to act at higher levels of perceived risk. A similar trend can be observed for tankers and cargo ships. To interpret the results, we need to clarify that the AMM is an indicator for judging whether the ship takes evasive action early or late. A ship acting early basically implies that the ship starts evasive action with a higher AMM. This does not mean that the action time is earlier. Compared with smaller vessel categories, the course changes of larger ships require more effort and time due to their relatively limited maneuverability. Let us take two ships as an example, one a small-size ship with better maneuverability and the other is a large-size ship with a relative lower maneuverability. Even though the starting action time of the smaller ship is slightly later than that of the larger ship in the same encounter scenario, if the AMM of the smaller ship is bigger than that of the larger ship, the smaller ship is regarded as acting earlier than the larger ship. Zhou et al. (2019) show that the behavioral characteristics of navigators of ships of different sizes are different. This may be a plausible explanation for the observation that larger vessels respond with a relative lower AMM to avoid a collision than smaller ships.

Third, the size of the risk perception-based SD varies by ship type, see Figures 8 and 9. The size of the risk perception-based SD of passenger ships is generally larger than that of the other two ship types. The safety of life has been the top priority for the passenger ship industry for decades, due to the huge threat of accidents and loss of human lives (Iqbal et al., 2008; Lu & Yang, 2011). This may be a reason why navigators on passenger ships have a low tolerance for conflict and take collision avoidance actions at lower levels of risk perception. Therefore, this may explain why the timing for a passenger ship to take an evasive maneuver is earlier. Further, when being as an SO, the risk perception-based SD's size for a tanker is larger than that for a cargo ship (Table 5). This indicates that the risk tolerance of a tanker that is the SO is lower than that of a cargo ship, as the tanker takes evasive maneuvers earlier than a cargo ship. We could explain this by taking into account ship maneuverability. The load conditions significantly influence a ship's maneuverability. The maneuverability of a fully loaded tanker is relatively poorer than that of a cargo ship, which directly reduces the AMM value of the tanker when an evasive maneuver starts.

5.2 Advantages of using AMM in the construction of risk perception-based SD

There are many concepts that can represent temporal closeness between a pair of vessels. TCPA is one of the most commonly used parameters because both spatial proximity and speed are integrated (Szlapczynski and Szlapczynska, 2017). TCPA represents the remaining time for two ships to reach their closest points if the course and speed remain the same.

The proposed risk perception-based SD based on the concept of AMM is more realistic than TCPA as the formulation of conflict based on the proposed risk perception-based SD is linked to conflict resolution. The risk solution presents the difficulty of performing evasive maneuvers to successfully avoid collisions. Determining the risk levels of conflict in ship-ship encounter situations independent of their potential for conflict resolution may lead to inaccurate detection of actual danger (Chen et al., 2018), considering that ship maneuverability helps to measure the level of risk more accurately (Baldauf et al., 2015; Huang and van Gelder, 2020). However, most of the existing research in terms of conflict based on TCPA ignore the impact of ship maneuverability.

Let us take the encounter scenarios in Figure 10 as an illustration. The only difference between them is the loaded condition of the GW. The half-loaded GW and fully loaded GW are marked in blue and red, respectively. The SD of the GW will be violated, so the conflict exists in both Figure 10(a) and Figure 10(b). Ship maneuverability affects this resolution solution (Hong and Yang, 2012). The load conditions significantly affect the ship maneuverability. Although the TCPA is the same for these two ship-pair encounter scenarios, their collision risk is different because the GW has different maneuverability. Therefore, the conflict analysis based on risk perception-based SD is more precise.

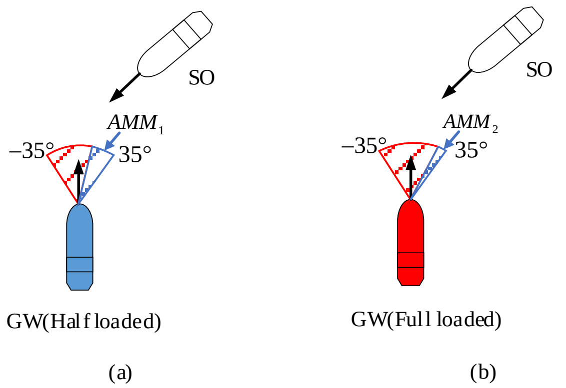

Figure 10 Ship conflict analysis based on risk perception-based SD

5.3 Application of risk perception-based Domain

The risk perception-based SD provides statistical information about the timing of a ship starting an evasive maneuver in terms of a perceived collision risk level. It shows how the navigators choose the timing to avoid the conflict in a specific area. The proposed risk perception-based SD based on the concept of AMM can be applied for the following purposes, although more work is needed to validate this application before practical implementation.

First, it can be used for providing information about waterway safety based on historic AIS data, such as near miss detection. Various methods have been proposed to analyze near misses from historical AIS data. One typical method measures the collision risk by obtaining insights into ship behavior characteristics during the process of collision avoidance. Any abnormal ship behavior during the process of collision avoidance normally leads to a serious encounter. Frenetic rudder actions may occur in the last moment before ship collision to prevent it happening (Mestl et al., 2016). The use of statistical techniques for detecting abnormal ship behavior has attracted increasing attention in maritime transportation research (Pallotta et al., 2013). The statistical characteristics of the risk perception-based SD in a given sea area can be obtained from a given AIS database. Then, abnormal behavior can be observed by comparing the AMM levels of encounters found in a new data time series to the normal risk perception-based SD determined earlier. When two ships approach each other and the give-way ship violates the risk perception-based SD, this means that the GW acts beyond normal operational conditions and probably approaches the boundaries of acceptable safety levels, since most ships (around 90% of the ships navigating in the area) would take evasive maneuvers before this moment. Combining the information derived from vessel encounters detected in AIS data in terms of risk perception-based SD violations, evasive maneuvers with other information about navigational safety can provide a comprehensive picture of the navigational safety levels in a given sea area. This can be done, for instance, by combining the risk perception-based SD with the ship's obligation for collision avoidance at different stages of the encounter as specified in the COLREGs, e.g., through a delineation of four safety levels, as specified in Du et al. (2020c, 2021).

Second, the risk perception-based SD could be further developed as a basis for a collision alert system onboard ships or in remote control centers. Real-time alerts for ship-ship encounter situations could significantly contribute to the reduction of collision accidents (Lehikoinen et al., 2015), and considerable work has been dedicated to proposing ship collision alert systems, see Gil et al. (2020). The proposed risk perception-based SD can be used as a basis for defining intelligent collision alerts, incorporating conflict resolution and comparing the characteristics of an ongoing encounter with historic patterns of normal operation in the area. When appropriate AMM threshold levels are used for raising alarms, such an intelligent collision alert system can reduce the number of unnecessary alarms, which is known to be a problem with existing collision alert systems (Baldauf et al. 2011).

Third, the risk perception-based SD could be used as a benchmark for testing the CAS in maritime autonomous surface ships (MASS), or for assessing the safety levels of introducing MASS in mixed traffic environments. The risk perception-based SD reflects the statistical features of the historically observed traffic flow. If the CAS in MASS can handle collision avoidance equally as well as human navigators, traffic flow with a mixed composition of MASS and conventional vessels would have similar statistical features to historically observed traffic flows. On the other hand, if the statistical features of the risk perception-based SD of the mixed traffic (MASS and conventional traffic) are different from the historic traffic characteristics, this would imply that the CAS in MASS might not perform as well as human navigators, and that mixed traffic would not be as safe as conventional vessel traffic. Thus, the risk perception-based SD could be used as a basis for simulation models to analyze safety levels under various traffic conditions, or as a benchmark when implementing MASS in real-world environments.

5.4 Limitations and future improvements

This work has introduced a risk perception-based SD and proposed a methodology for determining its shape and size. This was done by linking the timing of conflict elimination with the AMM as a proxy for collision risk levels perceived by a navigator. The maneuverability of the ship has been taken into account, measuring the capability of a vessel to eliminate the conflict. Although the results of the case studies and empirical findings are promising, several factors could further improve the proposed method and strengthen the findings and future applicability.

5.4.1 Ship maneuverability

The accuracy of modeling ship maneuverability also affects the accuracy of calculating a ship's AMM. The Nomoto model was employed in this work to measure ship maneuverability as it only requires limited input parameters. Although the Nomoto model is widely used as it is effective and comparatively simple, it may not be appropriate in some situations, e.g., for vessels with non-conventional steering arrangements. Ship maneuverability is improving significantly due to the fast development of the ship industry.

To measure the reliability of AMM computation based on the Nomoto model, a sensitivity analysis was conducted. 100 SPEEs were randomly selected to be the database for this sensitivity analysis. Figure 11 illustrates the impact of ship maneuverability on the value of AMM. There are two key parameters (i.e., K_0 and T_0) in the Nomoto model. For passenger and cargo ships, $K_0 = 1.5$ and $T_0 = 2.5$, and for tankers $K_0 = 1.5$ and $T_0 = 6$ (Hong & Yu, 2000). We varied K_0 and T_0 and checked how much the AMM varied relative to the baseline K_0 and T_0 values. Figure 11(a1-a8) shows the change in AMM when K is the only variable. Figure 11(b1-b8) shows the change in AMM when T is the only variable. The change rate of AMM (ΔAMM) is the magnitude of change in AMM divided by the reference value of AMM. The AMM with (K_0 , T_0) input was set as the reference. For instance, if the K_0 decreases by 0.1 and T remains the same, $\Delta AMM = (AMM(K_0 - 0.1, T_0) - AMM(K_0, T_0)) / AMM(K_0, T_0)$. In Figure 11, the x-axis is ΔAMM and the y-axis is the probability of ΔAMM ($P_{\Delta AMM}$).

The sensitivity analysis revealed the following three findings. First, AMM increases with an increase of K, but decreases with an increase of T. This is consistent with the fact that the combination of a large K and small T is a characteristic of excellent steering performance (Nomoto et al., 1956). A larger K means a large turning moment and a smaller T means a quick rudder response. The distribution of the ratio of ΔAMM is positively skewed when K increases or T decreases, however, it is negatively skewed when K decreases or T increases. $M_{\Delta AMM}$ is the mean value of ΔAMM . For example, when K increases by 0.1 and 0.4, $M_{\Delta AMM}$ increases by 0.012 and 0.035 respectively, see Figure 11. When T increases by 0.1 and 0.4, $M_{\Delta AMM}$ decreases by 0.003 and 0.011 respectively. Second, the impact of K on the AMM is higher than that of T. For instance, when K increases by 0.1, the increment of AMM is 0.012. When T increases by 0.1, the decrement of AMM is 0.003. Third, when the ship maneuvers with a higher AMM, the change in K and T has a minor impact on AMM. When the ship maneuvers late so that the AMM is low, the impact of K and T on AMM is more serious.

In brief, as many ships prefer to act early according to the statistical analysis in Section 4.4, the calculation of AMM is less affected by K and T. The $M_{\Delta AMM}$ is less than 6%, and therefore the calculation of AMM based on the Nomoto model is acceptable. Nonetheless, better information about the maneuverability characteristics of vessels could improve the definition of the risk perception-based SD. In future work, the MMG model (Tao et al., 2019) or Abkowitz's model (Zhang and Zou, 2011), which are more accurate than the Nomoto model, could be used to define a more accurate risk perception-based SD.

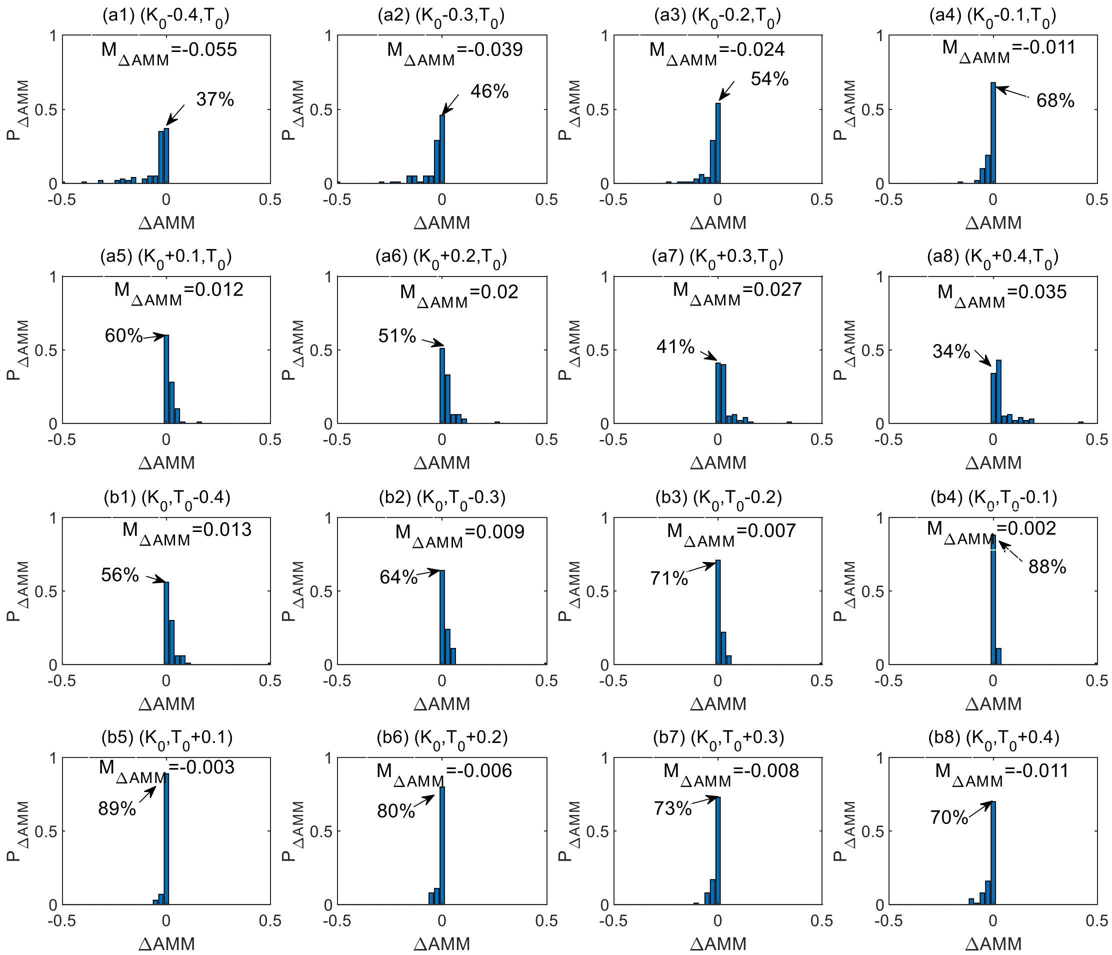

Figure 11. The impact of ship maneuverability on the value of AMM

5.4.2 Ship intention estimation

The intention estimation can be further improved, as it is a fundamental step for identifying a ship's evasive maneuvers. In this work, the intention is estimated from ship movement based on historical AIS data. However, ship movement is not only determined by the intention of the navigators but can also be influenced by several internal and external factors, such as wind and currents in ports and inland waterways (Zhou et al., 2020). Further addressing these influencing factors may be important for more accurate intention estimation. Additionally, when a ship encounters multiple targets, it is difficult to judge the intention of each action using AIS data alone. In this study, multi-vessel encounters were divided into multiple ship-pair encounters, and conflicts between multiple ships were not explicitly considered. This issue may lead to an inaccurate understanding of the action intention of the target ship (Du et al., 2020b).

5.4.3 Violation of COLREGs

Whether or not the ship action violates the COLREGs is not considered in this work. The ship domain proposed in this work is a data-driven model and the parameters were determined by historical data. The AIS data records what really happens during the collision avoidance process. From this study and other studies (Chauvin and Lardjane, 2008), the violation of COLREGs by the navigator does happen. For instance, the give-way ship may turn to portside for easy operation. Some safe navigators on board the SO prefer to act early to control the situation, whereas some risky navigators may choose to act late (Huang et al., 2020). However, this work only considered the conditions under which the ship took the first evasive action. We just reflect what really happened during the encounter process. Whether the behavior of a navigator complies with the COLREGs or not requires future work.

5.4.4 Size and shape of the proposed domain

The determination of the size and shape of the risk perception-based SD was simplified and can be further investigated. In this work, we simplified the shape of the risk perception-based SD to be a circular shape and its size was determined by choosing 90% as a threshold value for AMM. The circular shape of the SD is acceptable as a first analysis using this ship domain concept, but it is acknowledged that other researchers have proposed various irregular-shaped SDs such as ellipses or polygons (Pietrzykowski and Uriasz, 2009; Wang et al., 2010).

5.4.5 Other limitations

This work aims to make a conceptual proposal, rather than firm statements about the exact shape and size of the AMM-based ship domain. The algorithm designed to compute the AMM in this work is complex and in the current implementation takes a very long time to run. Therefore, only one-month AIS data is utilized to demonstrate the results. To propose the new concept, we believe one month of data is sufficient, but indeed for estimating the limits of the AMM-based domain accurately for a range of vessels, we acknowledge that one-month data is limited . More analyses with more data are needed in the future work, but as a prerequisite this work the current code of the algorithm needs to be optimized, or a meta-model needs to be developed to achieve a faster computation speed. This can help to increase the accuracy and reliability of the values obtained. As the current focus is to propose the concept of an AMM-based ship domain rather than defining its exact size and shape for a range of vessels, we leave this further development and more extensive data analysis for future work.

6. Conclusions

Existing ship domains are typically constructed based on the idea that navigators intend to keep an area around their vessel clear from other ships. With the realization that such proximity-based ship domains to assess navigational safety are limited, this article proposes a new ship domain concept and describes the empirical investigation of it. This risk perception-based ship domain (SD) was created on the timing of ships taking evasive maneuvers and the associated perceived risk levels. The boundary of this risk perception-based SD was empirically determined based on a large dataset of ship encounter situations detected in AIS data. Ship turning points were extracted through the Douglas–Peucker (DP) algorithm, after which the ship's evasive maneuver was estimated using the Non-Linear Velocity Obstacles (NLVO) algorithm. The concept of Available Maneuvering Margin (AMM) was employed to reflect the vessel's capability of conflict resolution, which is used as a proxy for the navigator's perceived collision risk at the timing of evasive maneuvering. This work helps explain and predict the behavior of ships in encounter situations with a potential ship-ship collision. The timing of the evasive maneuvers and the associated perceived risk levels were investigated, providing novel insights into maritime transport safety.

The results of the case study demonstrate that the proposed risk perception-based SD can give an understanding of the ship-ship collision avoidance process, indicating that the concept can be further developed in various applications to improve navigational safety. First, most navigators prefer to take evasive maneuvers early once collision dangers are detected. Second, the size of the risk perception-based SD is affected by many factors, indicating that navigators interpret and perceive collision risks differently in different encounter situations. Important factors in this interpretation include the ship length, ship type, and the ship COLREGs identity. The findings show that the timing of collision avoidance actions is delayed as ship lengths increases. The size of the risk perception-based SD of passenger ships is generally larger than that of tankers and cargo vessels. In terms of the ship COLREGs identity, it was found that the risk tolerance of a navigator of a tanker in 'stand-on' status is lower than those of navigators operating a cargo vessel with the same ship COLREGs identity. Third, as the dynamic nature of ship action and ship capability for conflict resolution are explicitly considered in this ship domain concept, we argue that this risk perception-based SD based on the concept of AMM has some advantages over Time to Closest Point of Approach (TCPA).

Based on our findings, we conclude that this SD concept can be further applied in various future developments, for instance, to provide information about maritime transportation safety based on historic AIS data (i.e., near miss detection), to develop intelligent collision alert systems, and to analyze the safety performance of maritime autonomous surface ships in future mixed traffic environments. However, more work is needed to validate this application before it is implemented. In light of the promising results of this SD concept, the proposed measurement procedure, and the obtained empirical findings, we would like to highlight several avenues for further development. These include the improvement of evasive maneuver estimation, a more advanced method to more accurately reflect vessels' maneuverability characteristics, and further integration and development of the proposed risk perception-based SD for waterway safety analysis and collision alert system development.

Acknowledgements

The first author of this work is supported by the China Scholarship Council (Grant Number: 201606950009) and Marine Technology research group in Aalto University (9170094). This work is also supported by the National Science Foundation of China (NSFC) through Grant No. 52001237. The work has further received financial support from the Canada First Research Excellence Fund, through the Ocean Frontier Institute. This financial support is gratefully acknowledged. Besides, we thank the two anonymous reviewers for their very insightful comments, which have been very instrumental to improve an earlier version of this work.

References

Asmi, E., Kivekäs, N., Kerminen, V. M., Komppula, M., Hyvärinen, A. P., Hatakka, J., ... & Lihavainen, H. (2011). Secondary new particle formation in Northern Finland Pallas site between the years 2000 and 2010. Atmospheric Chemistry & Physics Discussions, 11(9).

Aydogdu, Y. V., Yurtoren, C., Kum, S., Park, J. S., & Park, Y. S., 2010. Questionnaire survey on the risk perception in the Istanbul Strait. Journal of Navigation and Port Research, 34(7), 517-523.

Aydogdu, Y. V., 2014. A comparison of maritime risk perception and accident statistics in the Istanbul Straight. The Journal of Navigation, 67(1), 129.

Baldauf, M., Benedict, K., Fischer, S., Motz, F., & Schröder-Hinrichs, J. U., 2011. Collision avoidance systems in air and maritime traffic. Proceedings of the Institution of Mechanical Engineers, Part O: Journal of Risk and Reliability, 225(3), 333-343.

Baldauf, M., Mehdi, R., Deeb, H., Schröder-Hinrichs, J. U., Benedict, K., Krüger, C., ... & Gluch, M., 2015. Manoeuvring areas to adapt ACAS for the maritime domain. Zeszyty Naukowe Akademii Morskiej w Szczecinie.

Baldauf, M., Mehdi, R., Fischer, S., Gluch, M., 2017. A Perfect Warning to avoid collisions at sea? Sci. J. Maritime Univ. Szczecin 49 (121), 53–64.

Belcher, P., 2003. A day in the life of the Dover Strait. Safety at Sea International, 57(408), 15–16.

Chauvin, C., & Lardjane, S., 2008. Decision making and strategies in an interaction situation: Collision avoidance at sea. Transportation Research Part F: Traffic Psychology and Behaviour, 11(4), 259-269.

Chen, P., Huang, Y., Mou, J., & van Gelder, P. H. A. J. M., 2018. Ship collision candidate detection method: A velocity obstacle approach. Ocean Engineering, 170, 186-198.

Chin, H. C., & Debnath, A. K., 2009. Modeling perceived collision risk in port water navigation. Safety Science, 47(10), 1410-1416.

Coldwell, T. G., 1983. Marine traffic behaviour in restricted waters. The Journal of Navigation, 36(3), 430-444.

Conventions on the International Regulations for Preventing Collision at Sea (COLREGs). 1972. The International Maritime Organization (IMO).

Douglas, D.H., Peucker, T.K., 1973. Algorithms for the reduction of the number of points required to represent a digitized line or its caricature. Cartographica: The International Journal for Geographic Information and Geovisualization 10 (2), 112–122.

Du, L., Valdez Banda, O. A, & Kujala, P., 2019. An intelligent method for real-time ship collision risk assessment and visualization. In Developments in the Collision and Grounding of Ships and Offshore Structures: Proceedings of the 8th International Conference on Collision and Grounding of Ships and Offshore Structures (ICCGS 2019), 21-23 October, 2019, Lisbon, Portugal (p. 293). CRC Press.

Du, L., Goerlandt, F., Valdez Banda, O. A., Huang, Y., Wen Y., & Kujala, P., 2020a. Improving stand-on ship's situational awareness by estimating the intention of the give-way ship. Ocean Engineering, 201, 107110.

Du, L., Goerlandt, F., & Kujala, P., 2020b. Review and analysis of methods for assessing maritime waterway risk based on non-accident critical events detected from AIS data. Reliability Engineering & System Safety, 106933.

Du, L., Valdez Banda, O. A., Goerlandt, F., Huang, Y., & Kujala, P., 2020c. A COLREG-compliant ship collision alert system for stand-on vessels (In press).

Du, L., Valdez Banda, O. A., Goerlandt, F., Kujala, P., & Zhang, W., 2021. Improving Near Miss Detection in Maritime Traffic in the Northern Baltic Sea from AIS Data. Journal of Marine Science and Engineering, 9(2), 180.

EMSA, 2020. Annual overview of marine casualties and incidents 2020. European Maritime Safety Agency. Retrieved from: http://www.emsa.europa.eu/we-do/safety/accident-investigation/item/4266-annual-overview-of-marine-casualties-and-incidents-2020.html

Fan, C., Wróbel, K., Montewka, J., Gil, M., Wan, C., & Zhang, D., 2020. A framework to identify factors influencing navigational risk for Maritime Autonomous Surface Ships. Ocean Engineering, 202, 107188.

Fiskin, R., Nasiboglu, E., & Yardimci, M. O., 2020. A knowledge-based framework for two-dimensional (2D) asymmetrical polygonal ship domain. Ocean Engineering, 202, 107187.

Fujii, Y., & Tanaka, K., 1971. Traffic capacity. The Journal of navigation, 24(4), 543-552.

Gil, M., Wróbel, K., & Montewka, J., 2019. Toward a method evaluating control actions in STPA-based model of ship-ship collision avoidance process. Journal of Offshore Mechanics and Arctic Engineering, 141(5).

Gil, M., Montewka, J., Krata, P., Hinz, T., & Hirdaris, S., 2020. Determination of the dynamic critical maneuvering area in an encounter between two vessels: Operation with negligible environmental disruption. Ocean Engineering, 213, 107709.

Gil, M., Wróbel, K., Montewka, J., & Goerlandt, F., 2020. A bibliometric analysis and systematic review of shipboard Decision Support Systems for accident prevention. Safety science, 128, 104717.

Goodwin, E. M., 1975. A statistical study of ship domains. The Journal of navigation, 28(3), 328-344.

Goerlandt, F., Montewka, J., Kuzmin, V., & Kujala, P., 2015. A risk-informed ship collision alert system: framework and application. Safety Science, 77, 182-204.

Gucma, L., & Marcjan, K., 2012. Probabilistic model of minimal passing distances of vessels navigating in Polish coastal waters. 11th International Probabilistic Safety Assessment and Management Conference and the Annual European Safety and Reliability Conference 2012, PSAM11 ESREL 2012, 2012. 5536-5543.

Hansen, M. G., Jensen, T. K., Lehn-Schiøler, T., Melchild, K., Rasmussen, F. M., & Ennemark, F., 2013. Empirical ship domain based on AIS data. The Journal of Navigation, 66(6), 931-940.

Hörteborn, A., Ringsberg, J. W., Svanberg, M., & Holm, H., 2019. A Revisit of the Definition of the Ship Domain based on AIS Analysis. The Journal of Navigation, 72(3), 777-794.

Hong, B. & Yu Y., 2000. Ship's K, T indices statistics analysis. Journal of Dalian Maritime University, 26, 29-33.

Hong, B., & Yang, L., 2012. Ship handling. Dalian Maritime University Press, Dalian.

Huang, Y., & Gelder, P. H. A. J. M. V., 2017. Non-linear velocity obstacles with applications to the maritime domain. In 7th International Congress on Maritime Transportation and Harvesting of Sea Resources, Lisbon, Portugal.

Huang, Y., & van Gelder, P. H. A. J. M., 2020. Collision risk measure for triggering evasive actions of maritime autonomous surface ships. Safety science, 127, 104708.

Inoue, K., 2000. Evaluation method of ship-handling difficulty for navigation in restricted and congested waterways. The journal of navigation, 53(1), 167-180.

Iqbal, K. S., Bulian, G., Hasegawa, K., Karim, M. M., & Awal, Z. I., 2008. A rational analysis of intact stability hazards involving small inland passenger ferries in Bangladesh. Journal of marine science and technology, 13(3), 270-281.

Juszkiewicz, W., 2016. Verification of the accuracy requirements for relative course and closest point of approach. Zeszyty Naukowe/Akademia Morska w Szczecinie, (45 (117)), 108-113.

Kijima, K., & Furukawa, Y., 2003. Automatic collision avoidance system using the concept of blocking area. IFAC Proceedings Volumes, 36(21), 223-228.

Kim, D. H., 2020. Human factors influencing the ship operator's perceived risk in the last moment of collision encounter. Reliability Engineering & System Safety, 203, 107078.

Kujala, P., Hänninen, M., Arola, T., & Ylitalo, J., 2009. Analysis of the marine traffic safety in the Gulf of Finland. Reliability Engineering & System Safety, 94(8), 1349-1357.

Kulkarni, K., Goerlandt, F., Li, J., Banda, O. V., & Kujala, P., 2020. Preventing shipping accidents: Past, present, and future of waterway risk management with Baltic Sea focus. Safety Science, 129, 104798.

Lehikoinen, A., Hänninen, M., Storgård, J., Luoma, E., Mäntyniemi, S., & Kuikka, S., 2015. A Bayesian network for assessing the collision induced risk of an oil accident in the Gulf of Finland. Environmental science & technology, 49(9), 5301-5309.

Li, S., Liu, J., & Negenborn, R. R., 2019. Distributed coordination for collision avoidance of multiple ships considering ship maneuverability. Ocean Engineering, 181, 212-226.

Lu, C. S., & Yang, C. S., 2011. Safety climate and safety behavior in the passenger ferry context. Accident Analysis & Prevention, 43(1), 329-341.

Montewka, J., Hinz, T., Kujala, P., & Matusiak, J., 2010. Probability modelling of vessel collisions. Reliability Engineering & System Safety, 95(5), 573-589.

Montewka, J., & Przemyslak, K., 2014. Towards the assessment of a critical distance between two encountering ships in open waters. European Journal of Navigation, 12(3), 7-14.

Montewka, J., Gil, M., Wróbel, K., 2020. Discussion on the article by Zhang & Meng entitled "Probabilistic ship domain with applications to ship collision risk assessment" [Ocean Eng. 186 (2019) 106130]. Ocean Engineering 209, 107527. https://doi.org/10.1016/j.oceaneng.2020.107527

Montewka, J., Goerlandt, F., & Kujala, P., 2012. Determination of collision criteria and causation factors appropriate to a model for estimating the probability of maritime accidents. Ocean engineering, 40, 50-61.

Mou, J. M., Van der Tak, C., & Ligteringen, H., 2010. Study on collision avoidance in busy waterways by using AIS data. Ocean Engineering, 37(5-6), 483-490.

Nicholas, B., 2006. Risk perception and safety management systems in the global maritime industry. Policy and Practice in Health and Safety, 4(2), 59-75.

Nomoto, K., Taguchi, K., Honda, K., & Hirano, S., 1956. On the steering qualities of ships. Journal of Zosen Kiokai, 1956(99), 75-82.

Olsson, E., & Jansson, A., 2006. Work on the bridge–studies of officers on high-speed ferries. Behaviour & Information Technology, 25(1), 37-64.

Pallotta, G., Vespe, M., & Bryan, K., 2013. Vessel pattern knowledge discovery from AIS data: A framework for anomaly detection and route prediction. Entropy, 15(6), 2218-2245.

Pérez, F. L., & Clemente, J. A., 2007. The influence of some ship parameters on manoeuvrability studied at the design stage. Ocean Engineering, 34(3-4), 518-525.

Pietrzykowski, Z., 2008. Ship's fuzzy domain-a criterion for navigational safety in narrow fairways. The Journal of Navigation, 61(3), 499.

Pietrzykowski, Z., & Uriasz, J., 2009. The ship domain-a criterion of navigational safety assessment in an open sea area. The Journal of Navigation, 62(1), 93.

Robert, G., Hockey, J., Healey, A., Crawshaw, M., Wastell, D. G., & Sauer, J., 2003. Cognitive demands of collision avoidance in simulated ship control. Human factors, 45(2), 252-265.

Rong, H., Teixeira, A. P., & Soares, C. G., 2021. Spatial correlation analysis of near ship collision hotspots with local maritime traffic characteristics. Reliability Engineering & System Safety, 209, 107463.

Simsir, U., Amasyalı, M. F., Bal, M., Çelebi, U. B., & Ertugrul, S., 2014. Decision support system for collision avoidance of vessels. Applied Soft Computing, 25, 369-378.

Statheros, T., Howells, G., & Maier, K. M., 2008. Autonomous ship collision avoidance navigation concepts, technologies and techniques. The Journal of Navigation, 61(1), 129-142.

Szlapczynski, R., & Szlapczynska, J., 2016. An analysis of domain-based ship collision risk parameters. Ocean Engineering, 126, 47-56.

Szlapczynski, R., & Szlapczynska, J., 2017. Review of ship safety domains: Models and applications. Ocean Engineering, 145, 277-289.

Szlapczynski, R., Krata, P., & Szlapczynska, J., 2018. Ship domain applied to determining distances for collision avoidance manoeuvres in give-way situations. Ocean Engineering, 165, 43-54.

Tam, C., & Bucknall, R., 2010. Collision risk assessment for ships. Journal of marine science and technology, 15(3), 257-270.

Tao, J., Du, L., Dehmer, M., Wen, Y., Xie, G., & Zhou, Q., 2019. Path following control for towing system of cylindrical drilling platform in presence of disturbances and uncertainties. ISA transactions.

Valdez Banda, O. A., Goerlandt, F., Montewka, J., & Kujala, P., 2015. A risk analysis of winter navigation in Finnish sea areas. Accident Analysis & Prevention, 79, 100-116.

Valdez Banda, O. A., Kannos, S., Goerlandt, F., van Gelder, P. H., Bergström, M., & Kujala, P., 2019. A systemic hazard analysis and management process for the concept design phase of an autonomous vessel. Reliability Engineering & System Safety, 191, 106584.

Wang, N. 2010. An Intelligent Spatial Collision Risk Based on the Quaternion Ship Domain. Journal of Navigation, 63, 733-749.

Wielgosz, M., 2017. Ship domain in open sea areas and restricted waters: an analysis of influence of the available maneuvering area. TransNav: International Journal on Marine Navigation and Safety of Sea Transportation, 11.

Zhang, L., Meng, Q., Xiao, Z., & Fu, X., 2018. A novel ship trajectory reconstruction approach using AIS data. Ocean Engineering, 159, 165-174.

Zhang, L., & Meng, Q., 2019. Probabilistic ship domain with applications to ship collision risk assessment. Ocean Engineering, 186, 106130.

Zhang, M., Zhang, D., Goerlandt, F., Yan, X., & Kujala, P., 2019. Use of HFACS and fault tree model for collision risk factors analysis of icebreaker assistance in ice-covered waters. Safety science, 111, 128-143.

Zhang, W., Goerlandt, F., Kujala, P., & Wang, Y., 2016. An advanced method for detecting possible near miss ship collisions from AIS data. Ocean Engineering, 124, 141-156.

Zhang, W., Zou, Z., Wang, J., & Du, L., 2020. Multi-ship following operation in ice-covered waters with consideration of inter-ship communication. Ocean Engineering, 210, 107545.

Zhang, X. G., & Zou, Z. J., 2011. Identification of Abkowitz model for ship manoeuvring motion using ε-support vector regression. Journal of Hydrodynamics, 23(3), 353-360.

Zhao, J. S., Wu, Z. L. & Wang, F. C. 1993. Comments on Ship Domains. Journal of Navigation, 46, 422-436.

Zhao, L., & Shi, G., 2018. A method for simplifying ship trajectory based on improved Douglas–Peucker algorithm. Ocean Engineering, 166, 37-46.

Zhou, Y., Daamen, W., Vellinga, T., & Hoogendoorn, S. P., 2019. Ship classification based on ship behavior clustering from AIS data. Ocean Engineering, 175, 176-187.

Zhou, Y., Daamen, W., Vellinga, T., & Hoogendoorn, S. P., 2020. Impacts of wind and current on ship behavior in ports and waterways: A quantitative analysis based on AIS data. Ocean Engineering, 213, 107774.

Zhu, M., Sun, W., Hahn, A., Wen, Y., Xiao, C., & Tao, W., 2020. Adaptive modeling of maritime autonomous surface ships with uncertainty using a weighted LS-SVR robust to outliers. Ocean Engineering, 200, 107053.

Zhu, X., Xu, H., & Lin, J., 2001. Domain and its model based on neural networks. The Journal of Navigation, 54(1), 97-103..

Zhuo, Y., & Tang, T., 2008. An intelligent decision support system to ship anti-collision in multi-ship encounter. In 2008 7th World Congress on Intelligent Control and Automation (pp. 1066-1071). IEEE.

Appendix

Table 1. List of Abbreviations

AIS	Automatic Identification System	MDTC	Minimum Distance to Collision
AMM	Available Maneuvering Margin	NL-VO	Non-Linear VO
ARPA	Automated Radar Plotting Aid	OS	Own Ship
CAS	Collision Alert Systems	OT	Overtaking encounter
COLREGs	Convention on the International Regulations for Preventing Collisions at Sea	RB	Relative Bearing
CPA	closest point of approach	RH	Relative Heading
CR	Crossing encounter	SD	Ship Domain
DCPA	Distance at Closest Point of Approach	SF	Safe passing
DP algorithm	Douglas–Peucker algorithm	SO	Stand-on ship
SPEE	Ship-pair Encounter Event	TS	Target Ship
GW	Give-way ship	TCPA	Time to Closest Point of Approach
HO	Head-on encounter	TTC	Time to Collision
MASS	Maritime Autonomous Surface Ships	VO	Velocity Obstacles

Table 2. List of notations

AMM	the value of calculated AMM	t_1	the first time that ship take evasive maneuver
c	ship course	t_{SPEE}	time period of SPEE
h	ship heading	t_{ea}	the time of ship taking evasive maneuver

IC	conflict index	t_{ob}	observation time
K	turning ability index	t_r	the period that collision risk exists
Lon	longitude	t_{rs}	the starting moment of t_r
Lat	latitude	t_{re}	the ending moment of t_r
$M_{\Delta AMM}$	mean value of ΔAMM	t_{tp}	turning time
V_{TS}	TS's velocity	δ_s	the adopted rudder angle that can eliminate the existing collision risk
v	ship speed	δ_a	all available rudder angle
RV	reachable ship velocity	ΔC	the amount of course change
S_{NL_VO}	velocity obstacle zone at in TS's velocity space	ΔAMM	the change of AMM
T	turning lag index		